Weierstraß-Institut
für Angewandte Analysis und Stochastik
Leibniz-Institut im Forschungsverbund Berlin e. V.

Preprint ISSN 2198-5855

A posteriori error control for stationary coupled bulk-surface equations

Martin Eigel, Rüdiger Müller

submitted: December 16, 2015

Weierstrass-Institute
Mohrenstr. 39
10117 Berlin
Germany
E-Mail: Martin.Eigel@wias-berlin.de
Ruediger.Mueller@wias-berlin.de

No. 2196
Berlin 2015

2010 *Mathematics Subject Classification.* 65N30,65N15,58J32,65M15,74S05,65M60.

Key words and phrases. finite element method, a posteriori, error estimator, adaptive algorithm, surface finite elements, bulk-surface elliptic equations.

Edited by
Weierstraß-Institut für Angewandte Analysis und Stochastik (WIAS)
Leibniz-Institut im Forschungsverbund Berlin e. V.
Mohrenstraße 39
10117 Berlin
Germany

Fax: +49 30 20372-303
E-Mail: preprint@wias-berlin.de
World Wide Web: http://www.wias-berlin.de/

Abstract

We consider a system of two coupled elliptic equations, one defined on a bulk domain and the other one on the boundary surface. Problems of this kind of problem are relevant for applications in engineering, chemistry and in biology like e.g. biological signal transduction. For the a posteriori error control of the coupled system, a residual error estimator is derived which takes into account the approximation errors due to the finite element discretisation in space as well as the polyhedral approximation of the surface. An adaptive refinement algorithm controls the overall error. Numerical experiments illustrate the performance of the a posteriori error estimator and the proposed adaptive algorithm with several benchmark examples.

1 Introduction

Coupled reaction diffusion processes in the bulk and on the surface of some domain $\Omega \subset \mathbb{R}^d$, $d \in \{2, 3\}$, have recently attracted interest from an analytical point of view [ER13] and in different application areas such as biology, see e.g. [NGC$^+$07, RR12, GEW$^+$15]. In all these problems one has to simultaneously account for transport in normal as well as in tangential direction to the boundary surface whereas most often either only normal or only tangential phenomena are considered. We study a stationary prototype problem in a domain Ω with piecewise smooth boundary $\Gamma := \partial\Omega$ which can be decomposed into a finite set of N_Γ smooth surface patches $\{\Gamma^i\}_{i=1}^{N_\Gamma}$. We seek the solution $u : \Omega \to \mathbb{R}$ and $v : \Gamma \to \mathbb{R}$ of the stationary coupled diffusion-reaction problem

$$-\Delta u + u = f \qquad \text{in } \Omega, \tag{1.1a}$$

$$(\alpha u - \beta v) + \partial_n u = 0 \qquad \text{on } \cup_{i=1}^{N_\Gamma} \Gamma^i, \tag{1.1b}$$

$$-\Delta_\Gamma v + v + \partial_n u = g \qquad \text{on } \cup_{i=1}^{N_\Gamma} \Gamma^i, \tag{1.1c}$$

$$\nabla_\Gamma v \mid_{\Gamma^i} \cdot n_\Gamma^i + \nabla_\Gamma v \mid_{\Gamma^j} \cdot n_\Gamma^j = 0 \qquad \text{on } \partial\Gamma^i \cap \partial\Gamma^j \ . \tag{1.1d}$$

For each point on a surface patch Γ^i, n is the outer normal of Ω and ∇_{Γ^i} and Δ_Γ denote the tangential gradient and the Laplace-Beltrami operator, respectively. In the compatibility condition (1.1d), n_Γ^i denotes the outer normal of the patch Γ^i. For each point in $\partial\Gamma^i$, it lies in the tangent plane to Γ^i. The equation system (1.1) describes diffusive transport and reaction of a bulk species u and a surface species v which are coupled by some binding–unbinding process that transforms u to v by binding it to Γ and vice versa. For the sake of a convenient presentation, the diffusion coefficients and reaction rates are assumed to be 1 while the binding and unbinding rates are given by the positive constants α and β.

Existence and uniqueness of the solution to (1.1) have been proved in [ER13] for globally C^2 boundaries. Moreover, optimal a priori error estimates for finite element approximations of arbitrary order were derived for sufficiently smooth boundaries and data. For the time dependent version of (1.1), convergence to equilibrium and a-priori error estimates were shown in [EFPT15]. In [BHLZ14] a CutFEM method that uses the same volume grid to discretise both the volume and the surface equation is analysed. We complement the analysis of [ER13] by the derivation of an a posteriori error estimator for the error $e := (u - u_h, v - v_h)$ of a lowest order continuous FEM approximation (u_h, v_h) of the solution (u, v) of (1.1) measured in the energy norm. For this, we split the overall residual into an equilibration, a consistency and a data approximation residual. We transfer the classical residual error estimators for volume domains and for surfaces to the setting of the coupled system. While the a posteriori analyis for problems on polyhedral domains is rather mature, see e.g. [AO00, BR78, Ver96] and a priori analysis for finite elements on curved domains is well established, see e.g. [Sco73, Zlá73, Ber89] much less can be found for the a posteriori analysis on curved domains. Most notably, in [DR98], the focus is set on a very coarse domain approximation where large parts of the domain may not be discretised at all and the refinement algorithm has to explore and detect the necessary parts of the domain which are important for the discretisation. This is somehow opposite to the setting we are concerned with since due to the coupling to the surface equation, we expect the complete domain to be required for an accurate solution. Finite element methods on surfaces were analysed by [Dzi88] and [DD07]. In [BCMN13] a convergent refinement algorithm for surface finite elements is derived and quasi-optimality of the resulting discretisations is shown under certain assumptions. Our error estimator extends some of these results for the bulk-surface coupled equations. One main difficulty and contribution of this paper is the analysis of the geometry error of non-conformity caused by the polyhedral approximation of the surface manifold.

The outline of the paper is as follows: In Section 2, some notation regarding the involved domains and their approximations is introduced. Moreover, assumptions on the coefficients are clarified and the weak formulation and FEM discretisation of the problem is presented. In Section 3, we recall basic results from differential geometry which include integral transformations used later on. In particular, non-conformity estimates are derived which provide bounds for the error caused by the domain approximations. Section 4 is dedicated to the derivation of the residual a posteriori error estimator for the overall error which is the main result of this paper. It consists of a discretisation part and a geometric non-conformity part which both can be controlled a posteriori by computable indicators. Numerical experiments in Section 5 illustrate the performance of the derived a posteriori error estimator with several benchmark problems.

In order to simplify notation, we write $a \lesssim b$ if $a \leq C\, b$ with some mesh-independent positive constant C. Moreover, the common notation for Lebesgue and Sobolev spaces is employed.

2 Problem Formulation

We first introduce the weak formulation of (1.1) for some domain Ω and then formulate the corresponding discrete problem for a polyhedral domain Ω_h with a triangulation that interpolates Ω.

2.1 Weak formulation of the continuous problem

Let $\Omega \subseteq \mathbb{R}^d$ be a Lipschitz domain and $\Gamma = \partial\Omega$. Suppose Γ can be decomposed into $\Gamma = \bigcup_{i=1}^{N_\Gamma} \overline{\Gamma}^i$, where $\{\Gamma^i\}$ is a set of pairwise disjoint C^2 surfaces. Each boundary patch Γ^i is assumed to have a Lipschitz boundary $\partial\Gamma^i$. We introduce the spaces

$$U := H^1(\Omega), \tag{2.1a}$$

$$V := \{v \in L^2(\Gamma) : \nabla_\Gamma v \mid_{\Gamma^i} \in L^2(\Gamma^i),\ v \mid_{\Gamma^i} = v \mid_{\Gamma^j} \text{ on } \partial\Gamma^i \cap \partial\Gamma^j\} \tag{2.1b}$$

and denote their dual spaces by U^* and V^*, respectively. Moreover, we define the weak form of the Laplace-Beltrami operator $-\Delta_\Gamma : V \to \mathbb{R}$ such that for each $v \in V$ it holds

$$\int_\Gamma -\psi\, \Delta_\Gamma v \,\mathrm{d}s := \int_\Gamma \nabla_\Gamma \psi \cdot \nabla_\Gamma v \,\mathrm{d}s - \sum_{\Gamma^i=1}^{N_\Gamma} \int_{\partial\Gamma^i} \psi\, \nabla_\Gamma v \cdot n_\Gamma^i \,\mathrm{d}\sigma \qquad \text{for all } \psi \in V. \tag{2.2}$$

Note that in general the sum in (2.2) does not vanish because on $\bar{\Gamma}^i \cap \bar{\Gamma}^j$ $(i \neq j)$ the normal vectors n_Γ^i and n_Γ^j are not parallel unless Γ is a global C^1 surface. Therefore, the additional condition (1.1d) is necessary to recover from (2.2) the strong form of the Laplace-Beltrami operator for piecewise C^2 surfaces.

The weak form of (1.1) reads: Given $f \in U^*$ and $g \in V^*$, find $(u, v) \in U \times V$ such that, for all $(\phi, \psi) \in U \times V$,

$$\int_\Omega \nabla\phi \cdot \nabla u + \phi\, u \,\mathrm{d}x + \int_\Gamma \phi\,(\alpha u - \beta v)\,\mathrm{d}s = \int_\Omega \phi\, f \,\mathrm{d}x, \tag{2.3a}$$

$$\int_\Gamma \nabla_\Gamma\psi \cdot \nabla_\Gamma v + v\,\psi \,\mathrm{d}s - \int_\Gamma \psi\,(\alpha u - \beta v)\,\mathrm{d}s = \int_\Gamma \psi\, g \,\mathrm{d}s. \tag{2.3b}$$

This can also be written in the standard variational form

$$a((u, v), (\phi, \psi)) = \ell((\phi, \psi)) \qquad \text{for all } (\phi, \psi) \in U \times V, \tag{2.4}$$

with the bilinear and linear forms

$$a((u, v), (\phi, \psi)) := \alpha \int_\Omega \nabla\phi \cdot \nabla u + \phi\, u \,\mathrm{d}x + \beta \int_\Gamma \nabla_\Gamma\psi \cdot \nabla_\Gamma v + \psi\, v \,\mathrm{d}s \tag{2.5a}$$

$$+ \int_\Gamma (\alpha\phi - \beta\psi)(\alpha u - \beta v)\,\mathrm{d}s,$$

$$\ell((\psi, \phi)) := \alpha \int_\Omega \phi\, f \,\mathrm{d}x + \beta \int_\Gamma \psi\, g \,\mathrm{d}s. \tag{2.5b}$$

In an analogous way to [ER13], we easily verify that $a(\cdot, \cdot)$ is a continuous and coercive bilinear form on $U \times V$. Hence, the Lax-Milgram Theorem provides existence of a unique solution to (2.4).

2.2 Discrete Problem

Let $\Omega_h \subset \mathbb{R}^d$ be a polyhedral domain with the boundary $\Gamma_h = \partial\Omega_h$ and let $\mathcal{T}_h$ be a regular partition of Ω_h into simplices that interpolates Ω. For $d = 3$, we denote the sets of nodes, edges and faces of the triangulation $\mathcal{T}_h$ by $\mathcal{N}_h$, $\mathcal{E}_h$ and $\mathcal{F}_h$, respectively. If $d = 2$ we let $\mathcal{F}_h$ denote the set of edges and let $\mathcal{E}_h$ coincide with $\mathcal{N}_h$. The subset $\mathcal{F}_h^\partial := \{F_h \in \mathcal{F}_h : \ F_h \subset \Gamma_h\}$ defines a triangulation of Γ_h into $(d-1)$ dimensional simplices. Analogously to the volume, we introduce the sets of boundary edges and boundary nodes, denoted by $\mathcal{E}_h^\partial$ and $\mathcal{N}_h^\partial$. For each $T_h \in \mathcal{T}_h$, $F_h \in \mathcal{F}_h$, $E_h \in \mathcal{E}_h$, we set $h_T = \operatorname{diam}(T_h)$, $h_F = \operatorname{diam}(F_h)$, $h_E = \operatorname{diam}(E_h)$ and define by this the (global) mesh-size functions $h_\mathcal{T}$, $h_\mathcal{F}$, $h_\mathcal{E}$. The jump of some (piecewise) function $v \in L^2(\Omega;\mathbb{R}^d)$ over a face $F \in \mathcal{F}_h$ is defined by $[v]_F := v \cdot n_+ + v \cdot n_-$ where n_+, n_- denote the outer normals on $F = T_+ \cap T_-$ with respect to the elements $T_+, T_- \in \mathcal{T}_h$. If the normals are not continuous along faces, we use the notation $[[v]]_F$ to indicate this. Analogous definitions are assumed for jumps $[v]_E$ over edges $E \in \mathcal{E}_h$.

We introduce the spaces of continuous finite element functions

$$U_h := \left\{u_h \in C(\overline{\Omega_h}) \ : u_h|_{T_h} \in P_1(T_h) \quad \forall T_h \in \mathcal{T}_h\right\}, \tag{2.6a}$$

$$V_h := \left\{v_h \in C(\Gamma_h) \ : \ v_h|_{F_h} \in P_1(F_h) \quad \forall F_h \in \mathcal{F}_h^\partial\right\}, \tag{2.6b}$$

where P_1 is the space of piecewise polynomials of maximal degree one.

The discrete variational problem reads: Given $f_h \in U_h$ and $g_h \in V_h$, find $(u_h, v_h) \in U_h \times V_h$ such that

$$a_h((u_h, v_h), (\phi_h, \psi_h)) = \ell_h((\phi_h, \psi_h)) \qquad \text{for all } (\phi_h, \psi_h) \in U_h \times V_h \tag{2.7}$$

with the discrete bilinear and linear forms

$$a_h((u_h, v_h), (\phi_h, \psi_h)) := \alpha \int_{\Omega_h} \nabla\phi_h \cdot \nabla u_h + \phi_h u_h \,\mathrm{d}x + \beta \int_{\Gamma_h} \nabla_{\Gamma_h}\psi_h \cdot \nabla_{\Gamma_h} v_h + \psi_h v_h \,\mathrm{d}s \tag{2.8a}$$

$$+ \int_{\Gamma_h} (\alpha\phi_h - \beta\psi_h)(\alpha u_h - \beta v_h) \,\mathrm{d}s,$$

$$\ell_h((\phi_h, \psi_h)) := \alpha \int_{\Omega_h} \phi_h \, f_h \,\mathrm{d}x + \beta \int_{\Gamma_h} \psi_h \, g_h \,\mathrm{d}s. \tag{2.8b}$$

Existence and uniqueness of solutions to (2.7) can be proven by the Lax-Milgram Theorem, cf. [ER13]. Note that the finite element method defined above is non-conforming since U_h and V_h, in general are not subspaces of U and V. Moreover a_h and ℓ_h differ from a and ℓ since the integrals are defined over different domains.

3 Domain Approximation

When Ω is a curved domain, a triangulation $\mathcal{T}_h$ can not match the domain exactly. Instead, we require $\mathcal{T}_h$ to interpolate the boundary Γ and thereby to define an approximating polyhedral

domain Ω_h. Then, by application of some deformation which maps Ω_h to Ω, one can define an *exact triangulation* $\mathcal{T}$ of Ω consisting of curved elements such that $\Gamma = \partial\Omega$ is matched exactly. To refine $\mathcal{T}_h$, we apply a bisection of the volume elements with a subsequent projection of the new boundary nodes to Γ. For the construction of the exact triangulation to be well defined and for the analysis below, we need the following assumptions on the triangulation

- **(A1)** $\mathcal{T}_h$ interpolates Γ, i.e. the set of boundary nodes satisfies $\mathcal{N}_h^\partial \subset \Gamma$.
- **(A2)** $\mathcal{T}_h$ is sufficiently fine such that each boundary face $F_h \in \mathcal{F}_h^\partial$ or boundary edge $E_h \in \mathcal{E}_h^\partial$ is completely inside a narrow band wherein a nearest point projection to a boundary patch Γ^i is well defined.
- **(A3)** The non-smooth parts of Γ are mapped to boundary edges of $\mathcal{T}_h$, i.e. if $E_h \in \mathcal{E}_h^\partial$ then there is some $i \in \{1, \dots, N_\Gamma\}$ with $N_h \in \partial\Gamma^i$ for all nodes $N_h \in \mathcal{N}_h^\partial \cap E_h$.
- **(A4)** Each element $T_h \in \mathcal{T}_h$ has at most one boundary face $F_h \subseteq \partial\Omega_h \cap \partial T_h$.
- **(A5)** All refinements of $\mathcal{T}_h$ by bisection lead to a shape regular family of triangulations.

On polyhedral volume domains it is known that appropriate bisection algorithms guarantee the shape regularity and thus assumption **(A5)** is not necessary in this case. For the case of finite elements on curved surfaces we refer to the discussion in [DD07] and [BCMN13]. In the following sections, we always consider $\mathcal{T}_h$ as some refinement of a macro-triangulation without indicating the refinement level.

3.1 Approximation of curved elements

Given a curved element $T \in \mathcal{T}$, let $T_h \in \mathcal{T}_h$ be the simplex that interpolates the corner nodes of T. Let $\hat{T}$ denote the d-dimensional unit simplex. For each simplex $T_h \in \mathcal{T}_h$ there is an affine reference transformation which we refer to by $J : \hat{T} \to T_h$. The nonlinear reference transformation to T is denoted by $\mathcal{X}$. After rescaling to the unit simplex, the global bi-Lipschitz regularity of Γ implies that there is a constant $L > 0$ such that

$$hL^{-1}\,|z| \le \|\hat{\nabla}\mathcal{X}\,z\|_{L^2(T_h)} \le hL\,|z| \qquad \text{for all } z \in \mathbb{R}^d. \tag{3.1}$$

Due to the shape regularity assumption **(A5)**, there is a constant $L_h > 0$ such that

$$hL_h^{-1}\,|z| \le \|\hat{\nabla}J\,z\|_{L^2(T_h)} \le hL_h\,|z| \qquad \text{for all } z \in \mathbb{R}^d. \tag{3.2}$$

The domain Ω itself does not determine $\mathcal{X}$ in a unique way. In the literature, there are different appropriate constructions suggested, cf. [Sco73, Ber89, Dub90, ER13]. The basic concept is to describe the deformation of a flat surface or edge to the curved boundary and then extend this deformation into the volume.

For the construction of $\mathcal{X}$ we assume that if T_h has one boundary face $F_h \subset \mathcal{F}_h^\partial$ then J is such that $\hat{F} := \{\hat{x} \in \hat{T} : \hat{x}_d = 0\}$ is mapped to the boundary segment F_h as depicted in Fig. 1.

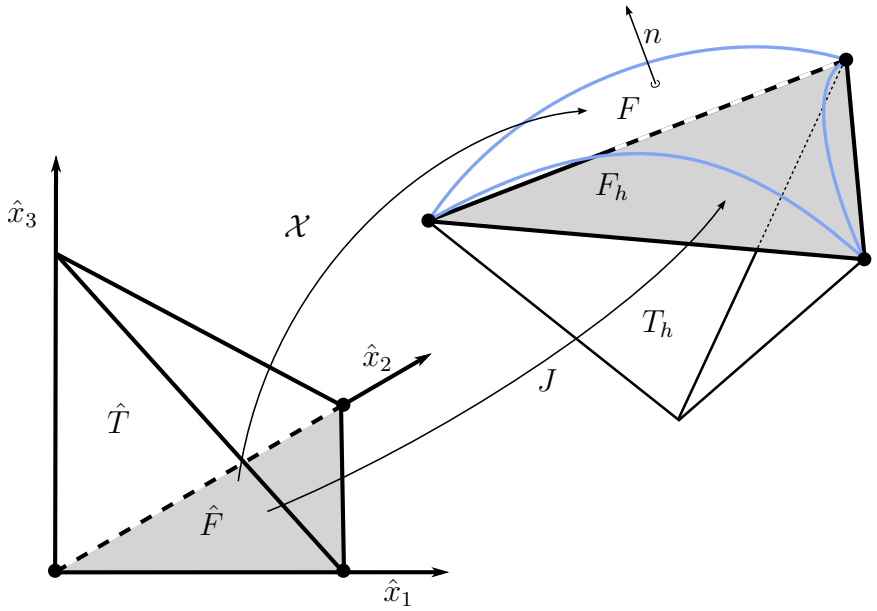

Figure 1: Transformation from reference element $\hat{T}$ to piecewise approximation Γ_h by $\mathcal{F}_h$ and to parametric representation Γ by P and $\mathcal{X}^i := P \circ \mathcal{F}_h$.

Analogously, if $T_h \cap \Gamma_h$ consists only of one boundary edge E_h, we assume that $E_h := J(\hat{E})$, where $\hat{E} := \{\hat{x} \in \hat{T} : \hat{x}_d = \hat{x}_{d-1} = 0\}$. Let $\mathcal{P}^i$ denote the nearest point projection from Γ_h^i to Γ^i. By **(A4)** and **(A2)**, $\mathcal{P}^i$ is well defined, and since each patch Γ^i is assumed to be C^2, we have that $\mathcal{P}^i$ is $C^1(\Gamma_h^i)$ [BCMN13]. Then, we define for all $\hat{x} \in \hat{T}$

$$\mathcal{X}(\hat{x}) = J(\hat{x}) + \begin{cases} \big[\mathcal{P}^i(J(\hat{x}_1, \dots, \hat{x}_{d-1}, 0)) - J(\hat{x}_1, \dots, \hat{x}_{d-1}, 0)\big] \rho_{\hat{F}}(\hat{x}_d) & \text{if } T \cap \Gamma = F, \\ \big[\mathcal{P}^i(J(\hat{x}_1, \dots, \hat{x}_{d-2}, 0, 0)) - J(\hat{x}_1, \dots, \hat{x}_{d-2}, 0, 0)\big] \rho_{\hat{E}}(\hat{x}_{d-1}, \hat{x}_d) & \text{if } T \cap \Gamma = E. \end{cases} \tag{3.3}$$

with $\rho_{\hat{F}}, \rho_{\hat{E}} \in C^1(\Omega)$ and $0 \leq \rho_{\hat{F}}, \rho_{\hat{E}} \leq 1$. The simplest choice for the extension of the boundary deformation into the element is $\rho_{\hat{F}}(x_d) = 1 - \hat{x}_d$ and $\rho_{\hat{E}}(x_{d-1}, x_d) = 1 - \hat{x}_{d-1} - \hat{x}_d$. By this approach, $\mathcal{X}$ is a C^1-diffeomorphism and without loss of generality we can assume that the Jacobi matrix $\hat{\nabla}\mathcal{X}$ is positive definite. Note that by the above construction a curved element $T \in \mathcal{T}$ can have more than one curved face if $d = 3$.

To quantify the deviation of a curved boundary face or edge from the polygonal interpolation, we define the *geometric element indicator*

$$\lambda_\Gamma(T_h) := h^{-1} \begin{cases} \|\hat{\nabla}_{\hat{F}}(\mathcal{X} - J)\|_{L^\infty(\hat{F})} & \text{if } T \cap \Gamma = F, \\ \|\hat{\nabla}_{\hat{E}}(\mathcal{X} - J)\|_{L^\infty(\hat{E})} & \text{if } T \cap \Gamma = E, \end{cases} \tag{3.4}$$

where $\hat{\nabla}_{\hat{F}}\Phi$ denotes the tangential gradient of Φ in $\hat{F}$ given by the first $d-1$ partial derivatives. Likewise, $\hat{\nabla}_{\hat{E}}\Phi$ is the tangential gradient in $\hat{E}$ subject to the first $d-2$ partial derivatives. Although $\lambda_\Gamma(T_h)$ is only defined on a boundary face or edge by (3.4), it in fact already characterises the difference between T and T_h completely:

Lemma 3.1. *For $T_h \in \mathcal{T}_h$ and $T \in \mathcal{T}$ the corresponding curved element, let $\mathcal{X}$ be defined according to* (3.3)*. Suppose there is one face $F \in \mathcal{F}^\partial$ or edge $E \in \mathcal{E}_h^\partial$ such that $T \cap \Gamma = F$ or $T \cap \Gamma = E$, respectively. There holds*

$$\|\hat{\nabla}(\mathcal{X} - J)\|_{L^\infty(\hat{T})} \lesssim h\, \lambda_\Gamma(T_h). \tag{3.5}$$

Proof. We assume $T \cap \Gamma = F$. The other case follows from analogous arguments. With the abbreviation $\Phi(\hat{x}_{\hat{F}}) := \mathcal{P}^i(J(\hat{x}_{\hat{F}}) - J(\hat{x}_{\hat{F}})$ for all $\hat{x}_{\hat{F}} \in \hat{F}$, we write

$$\hat{\nabla}(\mathcal{X} - J) = \Big(\rho_{\hat{F}}\, \hat{\nabla}_{\hat{F}}\Phi,\ \rho'_{\hat{F}}\,(\hat{x}_d)\Phi\Big)\,. \tag{3.6}$$

By the triangle inequality and since $0 \le \rho_{\hat{F}} \le 1$, we infer

$$\|\hat{\nabla}(\mathcal{X} - J)\|_{L^\infty(\hat{T})} \le \|\hat{\nabla}_{\hat{F}}\Phi\|_{L^\infty(\hat{F})} + \max_{\hat{x}\in\hat{T}} |\rho'_{\hat{F}}(\hat{x})|\, \|\Phi\|_{L^\infty(\hat{F})}. \tag{3.7}$$

Because T_h interpolates T, i.e. $\Phi(0) = 0$, and using that $\Phi(\hat{x}_{\hat{F}}) = \int_0^1 \hat{\nabla}_{\hat{F}}\Phi \cdot \hat{x}_{\hat{F}}\,\mathrm{d}s$, we conclude $\|\Phi\|_{L^\infty(\hat{F})} \le \|\hat{\nabla}_{\hat{F}}\Phi\|_{L^\infty(\hat{F})}$ to confirm the assertion. □

3.2 Basic differential geometry

For each boundary element $T \in \mathcal{T}$ or $T_h \in \mathcal{T}_h$, the partial derivatives of $\mathcal{X}$ or J with respect to $\hat{x}_1, \dots, \hat{x}_d$ build a complete set of linear independent tangential vectors to Γ or Γ_h, respectively. For $\hat{x} \in \hat{F}$ we define

$$\mathbb{T}(\hat{x}) := \hat{\nabla}_{\hat{F}}\mathcal{X}(\hat{x}) = [\hat{\partial}_1\mathcal{X}(\hat{x}), \cdots, \hat{\partial}_{d-1}\mathcal{X}(\hat{x})], \tag{3.8a}$$

$$\mathbb{T}_h(\hat{x}) := \hat{\nabla}_{\hat{F}}J \qquad = [\hat{\partial}_1 J, \cdots, \hat{\partial}_{d-1}J]. \tag{3.8b}$$

Then, the first fundamental form of Γ and Γ_h is given by the symmetric positive definite matrix

$$G = \mathbb{T}^T\mathbb{T} \qquad \text{and} \qquad G_h = \mathbb{T}_h^T\mathbb{T}_h, \tag{3.9}$$

respectively. Given $\hat{x} \in \hat{T}$ and $u \in U$, we set $\hat{u}(\hat{x}) := u \circ \mathcal{X}(\hat{x}) = u(x)$. Likewise, for $\hat{x}_{\hat{F}} \in \hat{F}$ and $v \in V$, we set $\hat{v}(\hat{x}_{\hat{F}}) := v \circ \mathcal{X}(\hat{x}_{\hat{F}}) = v(x_F)$. The gradients on $\hat{T}$ and $\hat{F}$ are related to respective gradients on Ω and Γ by

$$\hat{\nabla}\hat{u} = \nabla u\, \hat{\nabla}\mathcal{X} \quad \text{and} \quad \hat{\nabla}_{\hat{F}}\hat{v} = \nabla_\Gamma v\, \mathbb{T}. \tag{3.10}$$

With the change of variables formulas

$$\int_{\hat{T}} \hat{u}\, \det(\nabla\mathcal{X})\,\mathrm{d}\hat{x} = \int_{\mathcal{X}(\hat{T})} u\,\mathrm{d}x \quad \text{and} \quad \int_{\hat{F}} \hat{v}\,\sqrt{\det(G)}\,\mathrm{d}\hat{s} = \int_{\mathcal{X}(\hat{F})} v\,\mathrm{d}s \tag{3.11}$$

we get the identities

$$\int_{\hat{T}} \hat{\nabla}\hat{u}\cdot\hat{\nabla}\mathcal{X}^{-1}\hat{\nabla}\mathcal{X}^{-T}\hat{\nabla}\hat{u}\ \det(\nabla\mathcal{X})\,\mathrm{d}\hat{x} = \int_{\mathcal{X}(\hat{T})} \nabla u\cdot\nabla u\,\mathrm{d}x, \tag{3.12a}$$

$$\int_{\hat{F}} \hat{\nabla}_{\hat{F}}\hat{v}\cdot G^{-1}\hat{\nabla}_{\hat{F}}\hat{v}\,\sqrt{\det(G)}\,\mathrm{d}\hat{s} = \int_{\mathcal{X}(\hat{F})} \nabla_\Gamma v\cdot\nabla_\Gamma v\,\mathrm{d}s. \tag{3.12b}$$

Next, we want to get bounds for the perturbation of the transformation in terms of the geometric element indicator.

Lemma 3.2. *Let $T_h \in \mathcal{T}_h$ and $T \in \mathcal{T}$ be the corresponding curved element. Let $\mathcal{X}$, $\mathbb{T}$, G, and J, $\mathbb{T}_h$, G_h be defined as above. Suppose there is one face $F \in \mathcal{F}^\partial$ with $T \cap \Gamma = F$. Then,*

$$\|G - G_h\| \lesssim h^2 \lambda_\Gamma(T_h), \tag{3.13a}$$

$$|\det(G) - \det(G_h)| \lesssim h^{2d-2} \lambda_\Gamma(T_h) \tag{3.13b}$$

where $\|\cdot\|$ denotes a compatible matrix norm. Moreover, there holds

$$\left\| \frac{\sqrt{\det(G)}}{\sqrt{\det(G_h)}} - 1 \right\|_{L^\infty(\hat{F})} \lesssim \lambda_\Gamma(T_h), \tag{3.13c}$$

$$\left\| \mathbb{T}_h \left(\frac{\sqrt{\det G}}{\sqrt{\det G_h}} G^{-1} - G_h^{-1} \right) \mathbb{T}_h^T \right\|_{L^\infty(\hat{F})} \lesssim \lambda_\Gamma(T_h). \tag{3.13d}$$

Proof. For any $z \in \mathbb{R}^d$ it holds $z^T G z = \|\hat{\nabla}_{\hat{F}} \mathcal{X}\, z\|$ and hence the eigenvalues of G are bounded by $h^{-2}L^{-2}|z|^2 \leq z^T G z \leq h^{-2}L^2|z|^2$ due to (3.1). Analogously, we conclude that the eigenvalues of G_h lie in $[hL_h^{-1}, hL_h]$. We thus infer $\|\mathbb{T}\|_{L^2(\hat{F})}, \|\mathbb{T}_h\|_{L^2(\hat{F})} \lesssim h$ and $\det(G), \det(G_h) \lesssim h^{2d-2}$. By the definition of G, G_h and $\lambda_\Gamma(T_h)$, we obtain

$$\begin{aligned} \|G - G_h\| &= \|(\mathbb{T} - \mathbb{T}_h)^T \mathbb{T} + \mathbb{T}_h^T (\mathbb{T} - \mathbb{T}_h)\| \\ &\leq h \lambda_\Gamma(T_h)(\|\mathbb{T}\| + \|\mathbb{T}_h\|, \end{aligned} \tag{3.14}$$

which yields the first assertion. We use a Taylor expansion to deduce that there exists $0 \leq \theta \leq 1$ such that

$$\det(G) - \det(G_h) = \theta \big(D \det(G_h) \big)(G - G_h) \tag{3.15}$$

$$= \theta \det(G_h)\ \operatorname{trace}\left(G_h^{-1}(G - G_h) \right). \tag{3.16}$$

By Hölder's inequality we conclude that

$$|\det(G) - \det(G_h)| \lesssim |\det(G_h)|\, \|G_h^{-1}\|\, \|G - G_h\| \tag{3.17}$$

to infer (3.13b). For (3.13c), we note that

$$\sqrt{\det(G)} - \sqrt{\det(G_h)} = \frac{\det(G) - \det(G_h)}{\sqrt{\det(G)} + \sqrt{\det(G_h)}} \tag{3.18}$$

and that all powers of h cancel after division by $\det(G_h)$. Finally, using the abbreviations $q := \sqrt{\det(G)}$ and $q_h := \sqrt{\det(G_h)}$ leads to

$$\mathbb{T}_h \left(\frac{q}{q_h} G^{-1} - G_h^{-1} \right) \mathbb{T}_h^T = \mathbb{T}_h \left(\frac{q - q_h}{q_h} G^{-1} + G^{-1}(G_h - G) G_h^{-1} \right) \mathbb{T}_h^T. \tag{3.19}$$

The application of (3.13a) and (3.13c) now concludes the proof. □

Corollary 3.3. *Let $T_h \in \mathcal{T}_h$ and $T \in \mathcal{T}$ be the corresponding curved element. Let $\mathcal{X}$ and J be defined as above. We set $A := \hat{\nabla}\mathcal{X}^T\hat{\nabla}\mathcal{X}$ and $A_h := \hat{\nabla}J^T\hat{\nabla}J$. Suppose there is one face $F \in \mathcal{F}^\partial$ or edge $E \in \mathcal{E}_h^\partial$ such that $T \cap \Gamma = F$ or $T \cap \Gamma = E$, respectively. Then,*

$$\left\| \frac{\det(\hat{\nabla}\mathcal{X})}{\det(\hat{\nabla}J)} - 1 \right\|_{L^\infty(\hat{T})} \lesssim \lambda_\Gamma(T_h), \tag{3.20a}$$

$$\left\| \hat{\nabla}J \left(\frac{|\det \hat{\nabla}\mathcal{X}|}{|\det \hat{\nabla}J|} A^{-1} - A_h^{-1} \right) \hat{\nabla}J^T \right\|_{L^\infty(\hat{T})} \lesssim \lambda_\Gamma(T_h). \tag{3.20b}$$

Proof. With Lemma (3.1), the assertions follow from the same arguments as in Lemma 3.2. □

3.3 Lifts and geometric non-conformity estimates

We first define the lifting of functions defined on the curved domain or surface onto their corresponding polyhedral or polygonal discretisation and vice versa.

Definition 3.4. For functions $u_h : \Omega_h \to \mathbb{R}$ and $u : \Omega \to \mathbb{R}$ we define the lift and inverse lift by

$$u_h^\ell(\mathcal{X} \circ J^{-1}(x)) := u_h(x) \quad \text{and} \quad u^{-\ell}(x) := u_h(\mathcal{X} \circ J^{-1}(x)) \quad \text{for } x \in \Omega_h. \tag{3.21}$$

Likewise, for $v_h : \Gamma_h \to \mathbb{R}$ and $v : \Gamma \to \mathbb{R}$, we define

$$v_h^\ell(\mathcal{X} \circ J^{-1}(x)) := v_h(x) \quad \text{and} \quad v^{-\ell}(x) := v(\mathcal{X} \circ J^{-1}(x)) \quad \text{for } x \in \Gamma_h. \tag{3.22}$$

Next, we estimate the error which incurs due to integration on perturbed domains in order to compare functions on the curved domain and on its polyhedral approximation.

Lemma 3.5. *For $u_h^\ell, \phi \in U$ it holds*

$$\left| \int_\Omega u_h^\ell \, \phi \, \mathrm{d}x - \int_{\Omega_h} u_h \, \phi^{-\ell} \, \mathrm{d}x \right| \lesssim \sum_{T_h \in \mathcal{T}_h} \lambda_\Gamma(T_h) \, \|u_h\|_{L^2(T_h)} \, \|\phi^{-\ell}\|_{L^2(T_h)}, \tag{3.23a}$$

$$\left| \int_\Omega \nabla u_h^\ell \cdot \nabla \phi \, \mathrm{d}x - \int_{\Omega_h} \nabla u_h \cdot \nabla \phi^{-\ell} \, \mathrm{d}x \right| \lesssim \sum_{T_h \in \mathcal{T}_h} \lambda_\Gamma(T_h) \, \|\nabla u_h\|_{L^2(T_h)} \, \|\nabla \phi^{-\ell}\|_{L^2(T_h)}. \tag{3.23b}$$

Likewise, for $v_h^\ell, \psi \in V$ it holds

$$\left| \int_\Gamma v_h^\ell \, \psi \, \mathrm{d}s - \int_{\Gamma_h} v_h \, \psi^{-\ell} \, \mathrm{d}s \right| \lesssim \sum_{T_h \in \mathcal{T}_h} \lambda_\Gamma(T_h) \, \|v_h\|_{L^2(F_h)} \, \|\psi^{-\ell}\|_{L^2(F_h)}, \tag{3.23c}$$

$$\left| \int_\Gamma \nabla_\Gamma v_h^\ell \cdot \nabla_\Gamma \psi \, \mathrm{d}s - \int_{\Gamma_h} \nabla_{\Gamma_h} v_h \cdot \nabla_{\Gamma_h} \psi^{-\ell} \, \mathrm{d}s \right| \lesssim \sum_{T_h \in \mathcal{T}_h} \lambda_\Gamma(T_h) \, \|\nabla_\Gamma v_h\|_{L^2(F_h)} \, \|\nabla_\Gamma \psi^{-\ell}\|_{L^2(F_h)}. \tag{3.23d}$$

Proof. The identities follow from transformation to the reference domain and a pull-back. We start with the L^2 cases. By a localisation to elements and with (3.11) we derive

$$\begin{aligned}\int_T u_h^\ell \, \phi \,\mathrm{d}x - \int_{T_h} u_h \, \phi^{-\ell} \,\mathrm{d}x &= \sum_{T_h^i \in \mathcal{T}_h} \int_{\hat{T}} \hat{u}_h \left(|\det \hat{\nabla} \mathcal{X}^i| - |\det \hat{\nabla} J^i| \right) \hat{\phi} \,\mathrm{d}\hat{x} \\ &= \sum_{T_h^i \in \mathcal{T}_h} \int_{T_h^i} u_h \left(\frac{|\det \hat{\nabla} \mathcal{X}^i|}{|\det \hat{\nabla} J^i|} - 1 \right) \phi^{-\ell} \,\mathrm{d}x.\end{aligned}$$

Application of (3.20a) yields the assertions (3.23a). A similar argument and (3.13c) can be employed with the surface integral to get (3.23c). One can proceed in an analogous way for the H^1 cases. With (3.11) and (3.12), we obtain

$$\begin{aligned}&\int_T \nabla u_h^\ell \cdot \nabla \phi \,\mathrm{d}x - \int_{T_h} \nabla u_h \cdot \nabla \phi^{-\ell} \,\mathrm{d}x \\ &\qquad = \sum_{T_h^i \in \mathcal{T}_h} \int_{\hat{T}} \hat{\nabla} \hat{u}_h \left((A^i)^{-1} \, |\det \hat{\nabla} \mathcal{X}^i| - (A_h^i)^{-1} \, |\det \hat{\nabla} J^i| \right) \cdot \hat{\nabla} \hat{\phi} \,\mathrm{d}\hat{x} \\ &\qquad = \sum_{T_h^i \in \mathcal{T}_h} \int_{T_h^i} \nabla u_h \, \hat{\nabla} J^i \left(\frac{|\det \hat{\nabla} \mathcal{X}|}{|\det \hat{\nabla} J|} (A^i)^{-1} - (A_h^i)^{-1} \right) (\hat{\nabla} J^i)^T \cdot \nabla \phi^{-\ell} \,\mathrm{d}x.\end{aligned}$$

Application of (3.20b) yields the assertions (3.23b) and again similar arguments and (3.13d) can be employed with the surface integrals to get (3.23d). □

For sufficiently fine triangulations it is known that there is a norm equivalence for the lifting of functions in the volume, cf. [ER13] and on the surface, see [Dzi88, Dem09]. Here, we can get the equivalence from Lemma 3.5.

Lemma 3.6. *Assume the triangulation $\mathcal{T}_h$ is sufficiently fine such that the* global geometry estimator *satisfies*

$$\lambda_\Gamma := \max_{T_h \in \mathcal{T}_h} \lambda_\Gamma(T_h) \leq \lambda_0 < 1.$$

For $u \in H^1(\Omega)$ and $v \in H^1(\Gamma)$, it holds

$$\|u\|_{L^2(\Omega)} \approx \left\|u^{-\ell}\right\|_{L^2(\Omega_h)}, \qquad \|\nabla u\|_{L^2(\Omega)} \approx \left\|\nabla u^{-\ell}\right\|_{L^2(\Omega_h)}, \tag{3.24a}$$

$$\|v\|_{L^2(\Gamma)} \approx \left\|v^{-\ell}\right\|_{L^2(\Gamma_h)}, \qquad \|\nabla_\Gamma v\|_{L^2(\Gamma)} \approx \left\|\nabla_{\Gamma_h} v^{-\ell}\right\|_{L^2(\Gamma_h)}, \tag{3.24b}$$

where $a \approx b$ means $a \lesssim b$ and $b \lesssim a$.

Proof. Choosing $\phi = u_h^\ell$ in Lemma 3.5 yields

$$\left| \|u_h^\ell\|_{L^2(\Omega)}^2 - \|u_h\|_{L^2(\Omega_h)}^2 \right| \lesssim \lambda_\Gamma \, \|u_h\|_{L^2(\Omega_h)}^2. \tag{3.25}$$

It follows $\|u_h^\ell\|_{L^2(\Omega)}^2 \lesssim (1 + \lambda_\Gamma) \, \|u_h\|_{L^2(\Omega_h)}^2$ and $\|u_h\|_{L^2(\Omega_h)}^2 \lesssim (1 - \lambda_\Gamma)^{-1} \, \|u_h^\ell\|_{L^2(\Omega)}^2$. In an analogous way one can show (3.24b). □

4 Residual Error Estimation

This section is devoted to the derivation of a residual estimator of the error measured in the energy norm for the coupled problem. We introduce the energy norm on $U \times V$ by

$$\|\!|(\phi,\psi)|\!\|^2 := a((\phi,\psi),(\phi,\psi)) = \alpha \|\phi\|_U^2 + \beta \|\psi\|_V^2 + \|\alpha\phi - \beta\psi\|_{L^2(\Gamma)}^2 . \tag{4.1}$$

Given some finite element function $(u_h, v_h) \in U_h \times V_h$, the residual R with regard to the variational problem (2.4) is defined by

$$\langle R, (\phi,\psi)\rangle := a((u_h^\ell, v_h^\ell),(\phi,\psi)) - \ell(\phi,\psi) \quad \text{for all } (\phi,\psi) \in U \times V . \tag{4.2}$$

Proposition 4.1. *Let $(u,v) \in U \times V$ be the solution of* (2.4)*. Given $(u_h, v_h) \in U_h \times V_h$, the energy norm of the error satisfies*

$$|\!|\!|(u - u_h^\ell, v - v_h^\ell)|\!|\!| = \|R\|_* . \tag{4.3}$$

Proof. We set $e := (u_h^\ell - u, v_h^\ell - v)$ and easily check that for all $(\phi,\psi) \in U \times V$ we have $\langle R, (\phi,\psi)\rangle = a(e,(\phi,\psi))$. Hölder inequality directly implies $\langle R, (\phi,\psi)\rangle \le \|\!|e|\!\| \, |\!|\!|(\phi,\psi)|\!|\!|$ for all $(\phi,\psi) \in U \times V$ and thus $\|R\|_* \le \|\!|e|\!\|$. On the other hand, since $\langle R, e\rangle = \|\!|e|\!\|^2$, it follows

$$\|\!|e|\!\| = \frac{\langle R, e\rangle}{\|\!|e|\!\|} \le \sup_{w \in (U\times V)\setminus\{0\}} \frac{\langle R, w\rangle}{\|\!|w|\!\|} = \|R\|_* .$$

□

We split the residual into $R = R_h + R_{\text{nc}} + R_{\text{osc}}$ with

$$\langle R_h, (\phi,\psi)\rangle := a_h((u_h,v_h),(\phi^{-\ell},\psi^{-\ell})) - \ell_h(\phi^{-\ell},\psi^{-\ell}) , \tag{4.4a}$$

$$\begin{aligned}\langle R_{\text{nc}}, (\phi,\psi)\rangle := a((u_h^\ell, v_h^\ell),(\phi,\psi)) - a_h((u_h,v_h),(\phi^{-\ell},\psi^{-\ell})) \\ - \ell_h^\ell(\phi,\psi) \ + \ell_h(\phi^{-\ell},\psi^{-\ell}) ,\end{aligned} \tag{4.4b}$$

$$\langle R_{\text{osc}}, (\phi,\psi)\rangle := \ell_h^\ell(\phi,\psi) - \ell(\phi,\psi) . \tag{4.4c}$$

R_h is the discretisation part of the residual, R_{nc} is the non-conformity part which quantifies the quality of the polyhedral domain approximation Ω_h with respect to the exact domain Ω and R_{osc} is the data approximation part of the residual. In the subsequent sections, computable error bounds for R_h and R_{nc} are derived and then combined to yield the total a posteriori error estimate.

4.1 Discretisation residual

The derivation of the upper bound for the discretisation residual R_h largely follows the classical approach of residual error estimators, see e.g. [AO00, Ver96] and [CEHL12] for a recent account on the universal application of the principle. In the proof, we employ the stable interpolation

operator $\Pi_h : U^{-\ell} = H^1(\Omega_h) \to U_h$ of Scott and Zhang [SZ90]. For $\phi \in H^1(\Omega_h)$ and any $T_h \in \mathcal{T}_h$, $F_h \in \mathcal{F}_h$, it verifies

$$\|\phi - \Pi_h\phi\|_{L^2(T_h)} \lesssim h_T \|\nabla\phi\|_{L^2(\omega_{T_h})}, \tag{4.5a}$$

$$\|\phi - \Pi_h\phi\|_{L^2(F_h)} \lesssim h_F^{1/2} \|\nabla\phi\|_{L^2(\omega_{F_h})}, \tag{4.5b}$$

where ω_{T_h} and ω_{F_h} denote patches containing T_h or F_h, respectively, and all neighbouring elements. In an analogous way, we introduce the stable interpolation operator $\Pi_h^\partial : V^{-\ell} \to V_h$ on the polyhedral boundary Γ_h. It holds

$$\left\|\psi - \Pi_h^\partial\psi\right\|_{L^2(F_h)} \lesssim h_F \|\nabla_{\Gamma_h}\psi\|_{L^2(\omega^\partial_{F_h})}, \tag{4.6a}$$

$$\left\|\psi - \Pi_h^\partial\psi\right\|_{L^2(E_h)} \lesssim h_E^{1/2} \|\nabla_{\Gamma_h}\psi\|_{L^2(\omega^\partial_{E_h})}, \tag{4.6b}$$

with surface patches $\omega^\partial_{F_h} \subset \Gamma_h$ and $\omega^\partial_{E_h} \subset \Gamma_h$.

Lemma 4.2. *Let $(u_h, v_h) \in U_h \times V_h$ be a solution of the discrete problem* (2.7)*. For all $(\phi, \psi) \in U \times V$, the discretisation residual R_h satisfies the estimate*

$$\langle R_h, (\phi, \psi)\rangle \lesssim \alpha\,(\eta_B + \eta_C)\,\|\nabla\phi\|_{L^2(\Omega)} + \beta\,\eta_S\,\|\nabla_\Gamma\psi\|_{L^2(\Gamma)}, \tag{4.7}$$

where the error indicators on the right-hand side are given by

$$\eta_C := \left\|h_{\mathcal{F}_h^\partial}^{1/2}(\alpha u_h - \beta v_h + \partial_n u_h)\right\|_{L^2(\mathcal{F}_h^\partial)}, \tag{4.8a}$$

$$\eta_B := \|h_{\mathcal{T}_h}(\Delta u_h - u_h + f_h)\|_{L^2(\mathcal{T}_h)} + \left\|h_{\mathcal{F}_h}^{1/2}[\partial_n u_h]_{\mathcal{F}_h}\right\|_{L^2(\mathcal{F}_h\setminus\mathcal{F}_h^\partial)}, \tag{4.8b}$$

$$\eta_S := \left\|h_{\mathcal{F}_h^\partial}(\Delta_{\Gamma_h} v_h - (1+\beta)v_h + \alpha u_h + g_h)\right\|_{L^2(\mathcal{F}_h^\partial)} + \left\|h_{\mathcal{E}_h^\partial}^{1/2}[[\partial_n v_h]]_{\mathcal{E}^\partial}\right\|_{L^2(\mathcal{E}_h^\partial)}. \tag{4.8c}$$

Here, the discrete norms are defined as summation over the elements or faces, respectively. By $[\partial_n u_h]_{\mathcal{F}_h}$ we denote the usual jump of the normal derivative at element faces and $[[\partial_n v_h]]_{\mathcal{E}^\partial}$ is the corresponding jump quantity on the surface defined as in (1.1d)*.*

Proof. Let $(\phi, \psi) \in U \times V$, then $(\Pi_h\phi^{-\ell}, \Pi_h^\partial\psi^{-\ell}) \in U_h \times V_h$ is in the kernel of R_h. Thus, a splitting of R_h into element contributions and an integration by parts result in

$$\begin{aligned}
\langle R_h, (\phi, \psi)\rangle = \alpha \sum_{T_h\in\mathcal{T}_h} \Bigg(&\int_{T_h} (-\Delta u_h + u_h - f_h)(\phi^{-\ell} - \Pi_h\phi^{-\ell})\,\mathrm{d}x \\
&+ \sum_{F_h\in\partial T_h} \int_{F_h} \partial_n u_h(\phi^{-\ell} - \Pi_h\phi^{-\ell})\,\mathrm{d}s\Bigg) \\
+ \alpha \sum_{F_h\in\mathcal{F}_h^\partial} &\int_{F_h} (\alpha u_h - \beta v_h)(\phi^{-\ell} - \Pi_h\phi^{-\ell})\,\mathrm{d}s \\
+ \beta \sum_{F_h\in\mathcal{F}_h^\partial} \Bigg(&\int_{F_h} (-\Delta_{\Gamma_h} v_h + (1+\beta)v_h - \alpha u_h - g_h)(\psi^{-\ell} - \Pi_h^\partial\psi^{-\ell})\,\mathrm{d}s \\
&+ \sum_{E_h\in\partial F_h} \int_{E_h} \partial_n v_h(\psi^{-\ell} - \Pi_h^\partial\psi^{-\ell})\,\mathrm{d}\sigma\Bigg).
\end{aligned} \tag{4.9}$$

In the sum over all $T_h \in \mathcal{T}_h$ we collect all contributions over the inner faces $F_h \in \mathcal{F}_h \setminus \mathcal{F}_h^\partial$ and move the boundary face parts to the coupling term. The Cauchy-Schwarz inequality yields

$$\begin{aligned}
\langle R_h, (\phi,\psi)\rangle \lesssim\ & \alpha \sum_{T_h\in\mathcal{T}_h} \|\Delta u_h - u_h + f_h\|_{L^2(T_h)} \left\|\phi^{-\ell} - \Pi_h\phi^{-\ell}\right\|_{L^2(T_h)} \\
& + \alpha \sum_{F_h\in\mathcal{F}_h\setminus\mathcal{F}_h^\partial} \|[\partial_n u_h]_{\mathcal{F}_h}\|_{L^2(F_h)} \left\|\phi^{-\ell} - \Pi_h\phi^{-\ell}\right\|_{L^2(F_h)} \\
& + \alpha \sum_{F_h\in\mathcal{F}_h^\partial} \|\alpha u_h - \beta v_h + \partial_n u_h\|_{L^2(F_h)} \left\|\phi^{-\ell} - \Pi_h\phi^{-\ell}\right\|_{L^2(F_h)} \qquad (4.10) \\
& + \beta \sum_{F_h\in\mathcal{F}_h^\partial} \|\Delta_{\Gamma_h} v_h - (1+\beta)v_h + \alpha u_h + g_h\|_{L^2(F_h)} \left\|\psi^{-\ell} - \Pi_h^\partial\psi^{-\ell}\right\|_{L^2(F_h)} \\
& + \beta \sum_{E_h\in\mathcal{E}_h^\partial} \left\|[[\partial_n v_h]]_{\mathcal{E}_h^\partial}\right\|_{L^2(E_h)} \left\|\psi^{-\ell} - \Pi_h^\partial\psi^{-\ell}\right\|_{L^2(E_h)}.
\end{aligned}$$

Then the properties of the interpolation (4.5) and (4.6) and the the norm equivalence of the lifted functions according to Lemma 3.6 complete the proof. □

4.2 Non-conformity residual

The geometric element indicator $\lambda(T)$ and the comparison results of Sect. 3 lead to an upper bound for R_{nc} which is due to the polyhedral approximation of the curved domain Ω.

Lemma 4.3. *Assume the triangulation $\mathcal{T}_h$ is sufficiently fine such that Lemma 3.6 holds. For any $(\phi,\psi) \in U \times V$, the non-conformity residual R_{nc} satisfies*

$$\begin{aligned}
\langle R_{nc}, (\phi,\psi)\rangle \lesssim\ & \eta_{nc}^{B,0}\|\phi\|_{L^2(\Omega)} + \eta_{nc}^{B,1}\|\nabla\phi\|_{L^2(\Omega)} + \eta_{nc}^{C}\|\alpha\phi - \beta\psi\|_{L^2(\Gamma)} \\
& + \eta_{nc}^{S,0}\|\psi\|_{L^2(\Gamma)} + \eta_{nc}^{S,1}\|\nabla_\Gamma\psi\|_{L^2(\Gamma)},
\end{aligned}$$

where the element indicators are given by

$$\eta_{nc}^{B,0} := \alpha \sum_{T_h\in\mathcal{T}_h} \lambda_\Gamma(T_h)\,\|u_h - f_h\|_{L^2(T_h)}, \qquad (4.11a)$$

$$\eta_{nc}^{B,1} := \alpha \sum_{T_h\in\mathcal{T}_h} \lambda_\Gamma(T_h)\,\|\nabla u_h\|_{L^2(T_h)}, \qquad (4.11b)$$

$$\eta_{nc}^{C} := \sum_{F_h\in\mathcal{F}_h^\partial} \lambda_\Gamma(F_h)\,\|\alpha u_h - \beta v_h\|_{L^2(F_h)}, \qquad (4.11c)$$

$$\eta_{nc}^{S,0} := \beta \sum_{F_h\in\mathcal{F}_h^\partial} \lambda_\Gamma(F_h)\,\|v_h - g_h\|_{L^2(F_h)}, \qquad (4.11d)$$

$$\eta_{nc}^{S,1} := \beta \sum_{F_h\in\mathcal{F}_h^\partial} \lambda_\Gamma(F_h)\,\|\nabla_{\Gamma_h} v_h\|_{L^2(F_h)}. \qquad (4.11e)$$

Proof. Let $(\phi,\psi)\in U\times V$. We rearrange terms to split $\langle R_{\mathrm{nc}},(\phi,\psi)\rangle = \mathcal{I}_B+\mathcal{I}_S+\mathcal{I}_C$ with

$$\mathcal{I}_B = \alpha\bigg(\int_\Omega \nabla u_h^\ell\cdot\nabla\phi + (u_h^\ell - f_h^\ell)\phi\,\mathrm{d}x - \int_{\Omega_h}\nabla u_h\cdot\nabla\phi^{-\ell}+(u_h-f_h)\phi^{-\ell}\,\mathrm{d}x\bigg),$$
$$\mathcal{I}_S = \beta\bigg(\int_\Gamma \nabla_\Gamma v_h^\ell\cdot\nabla_\Gamma\psi + \big(v_h^\ell-g_h^\ell\big)\psi\,\mathrm{d}s - \int_{\Gamma_h}\nabla_{\Gamma_h}v_h\cdot\nabla_{\Gamma_h}\psi^{-\ell}+\big(v_h-g_h\big)\psi^{-\ell}\,\mathrm{d}s\bigg),$$
$$\mathcal{I}_C = \bigg(\int_\Gamma(\alpha u_h^\ell-\beta v_h^\ell)(\alpha\phi-\beta\psi)\,\mathrm{d}s - \int_{\Gamma_h}(\alpha u_h-\beta v_h)(\alpha\phi^{-\ell}-\beta\psi^{-\ell})\,\mathrm{d}s\bigg).$$

To estimate the coupling term $\mathcal{I}_C$, we split the integral into its contributions from the surface elements and apply (3.11) and Lemma 3.5. This yields

$$\begin{aligned}\mathcal{I}_C &= \alpha\sum_{F_h\in\mathcal{F}_h^\partial}\int_{F_h}\left(\frac{\sqrt{\det(G)}}{\sqrt{\det(G_h)}}-1\right)(\alpha u_h-\beta v_h)(\alpha\phi^{-\ell}-\beta\psi^{-\ell})\,\mathrm{d}s\\ &\lesssim \alpha\sum_{F_h\in\mathcal{F}_h^\partial}\lambda_\Gamma(T_h)\,\|\alpha u_h-\beta v_h\|_{L^2(F_h)}\,\|\alpha\phi^{-\ell}-\beta\psi^{-\ell}\|_{L^2(\Gamma_h)}\end{aligned}$$

In an analogous way, we estimate the surface part $\mathcal{I}_S$ where we also use (3.12) for the gradient terms. It follows

$$\begin{aligned}\mathcal{I}_S &= \beta\sum_{F_h\in\mathcal{F}_h^\partial}\int_{F_h}\nabla v_h\left(\frac{\sqrt{\det(G)}}{\sqrt{\det(G_h)}}\mathbb{T}\left(G^{-1}-G_h^{-1}\right)\mathbb{T}^T\right)\cdot\nabla\psi^{-\ell}\,\mathrm{d}s\\ &\quad+\beta\sum_{F_h\in\mathcal{F}_h^\partial}\int_{F_h}\left(\frac{\sqrt{\det(G)}}{\sqrt{\det(G_h)}}-1\right)\big(v_h-g_h\big)\psi^{-\ell}\,\mathrm{d}s\\ &\lesssim \beta\sum_{F_h\in\mathcal{F}_h^\partial}\lambda_\Gamma(T_h)\left(\|\nabla v_h\|_{L^2(F_h)}\,\|\nabla\psi^{-\ell}\|_{L^2(\Gamma_h)}+\|v_h-g_h)\|_{L^2(F_h)}\,\|\psi^{-\ell}\|_{L^2(\Gamma_h)}\right)\end{aligned}$$

Likewise, the bulk term can be bounded by

$$\mathcal{I}_B\lesssim\alpha\sum_{T_h\in\mathcal{T}_h}\lambda_\Gamma(T_h)\left(\|\nabla u_h\|_{L^2(T_h)}\,\|\nabla\phi^{-\ell}\|_{L^2(\Omega_h)}\,+\|u_h-f_h\|_{L^2(T_h)}\,\|\phi^{-\ell}\|_{L^2(\Omega_h)}\right).$$

Application of Lemma 3.6 completes the proof. □

4.3 Overall error estimator

As a direct consequence of the preceding Sects. 4.1 and 4.2, we devise an a posteriori estimator for the overall error of a finite element solution of the coupled problem and prove its reliability and efficiency. In the subsequent error analysis, we employ piecewise constant approximations of the data. We define $f_h:\Omega_h\to\mathbb{R}$ by $f_h|_{T_h}=|T_h|^{-1}\int_{T_h}f^{-\ell}\,\mathrm{d}x$ for each $T_h\in\mathcal{T}_h$. The

oscillations of the data f and g are defined by

$$\operatorname{osc}(f,T_h) := h_{T_h}\left\|f^{-\ell}-f_h\right\|_{L^2(T_h)} \qquad \text{and} \quad \operatorname{osc}(f,\mathcal{T}_h) := \sum_{T_h\in\mathcal{T}_h}\operatorname{osc}(f,T_h), \tag{4.12a}$$

$$\operatorname{osc}(g,F_h) := h_{F_h}\left\|g^{-\ell}-g_h\right\|_{L^2(F_h)} \qquad \text{and} \quad \operatorname{osc}(g,\mathcal{F}_h^\partial) := \sum_{F_h\in\mathcal{F}_h^\partial}\operatorname{osc}(g,F_h). \tag{4.12b}$$

Theorem 4.4. *Assume the triangulation $\mathcal{T}_h$ is sufficiently fine such that Lemma 3.6 holds. For the solution $(u_h,v_h)\in U_h\times V_h$ of the discrete problem* (2.7)*, it holds*

$$\left|\!\left|\!\left|(u-u_h^\ell,v-v_h^\ell)\right|\!\right|\!\right| \lesssim \eta_h+\eta_{nc}+\operatorname{osc}_h, \tag{4.13}$$

$$\eta_h \lesssim \left|\!\left|\!\left|(u-u_h^\ell,v-v_h^\ell)\right|\!\right|\!\right| + \eta_{nc}+\operatorname{osc}_h, \tag{4.14}$$

with the discretisation error indicator of (4.8) *and the non-conformity indicator according to* (4.11)

$$\begin{aligned}\eta_h &:= \eta_B+\eta_C+\eta_S,\\ \eta_{nc} &:= h_{\mathcal{T}}\eta_{nc}^{B,0}+\eta_{nc}^{B,1}+h_{\mathcal{F}^\partial}\eta_{nc}^{S,0}+\eta_{nc}^{S,1}+\eta_{nc}^{C},\end{aligned}$$

and data oscillations $\operatorname{osc}_h := \operatorname{osc}(f,\mathcal{T}_h)+\operatorname{osc}(g,\mathcal{F}_h)$.

Proof. We easily verify that for all $(\phi,\psi)\in U\times V$ it holds

$$\begin{aligned}\langle R_{\mathrm{osc}},(\phi,\psi)\rangle &\lesssim \sum_{T\in\mathcal{T}}\left\|f_h^\ell-f\right\|_{L^2(T)}\|\phi\|_{L^2(T)}+\sum_{F\in\mathcal{F}^\partial}\left\|g_h^\ell-g\right\|_{L^2(T)}\|\psi\|_{L^2(F)}\\ &\lesssim \sum_{T_h\in\mathcal{T}_h} h_{T_h}\left\|f_h-f^{-\ell}\right\|_{L^2(T_h)}\left\|\nabla\phi^{-\ell}\right\|_{L^2(T_h)}\\ &\quad+\sum_{F_h\in\mathcal{F}_h^\partial} h_{F_h}\left\|g_h-g^{-\ell}\right\|_{L^2(T_h)}\left\|\nabla_\Gamma\psi^{-\ell}\right\|_{L^2(F_h)}.\\ &\lesssim \sum_{T_h\in\mathcal{T}_h}\operatorname{osc}(f,T_h)\|\nabla\phi\|_{L^2(\Omega)}+\sum_{F_h\in\mathcal{F}_h^\partial}\operatorname{osc}(g,F_h)\|\nabla_\Gamma\psi\|_{L^2(\Gamma)}.\end{aligned}$$

Then, the first part (reliability) is an immediate consequence of Lemmas 4.2 and 4.3. To prove efficiency, we apply the standard technique due to Verfürth. We have to consider all terms contributing to the indicator η_h and thus carry out the proof in several steps.

i) Efficiency of η_B For any $T_h\in\mathcal{T}_h$ and for any $F_h\in\mathcal{F}_h$, we introduce the (volume) bubble functions b_{T_h} and b_{F_h} with $\operatorname{supp} b_{T_h}=T_h$ and $\operatorname{supp} b_{F_h}=\omega_{F_h}$, where ω_{F_h} consists of the elements adjacent to F_h. The bubble functions are normalized such that $\max_{x\in T_h} b_{T_h}(x)=1$ and $\max_{x\in F_h} b_{F_h}(x)=1$. For any $T_h\in\mathcal{T}_h$ and $F_h\in\mathcal{F}_h$, let

$$\begin{aligned} r_{T_h}^B &:= \Delta u_h-u_h+f_h, & r_{F_h}^B &:= [\partial_n u_h],\\ \phi_{T_h} &:= b_{T_h}\, r_{T_h}^B, & \phi_{F_h} &:= b_{F_h}\, r_{F_h}^B.\end{aligned}$$

By the equivalence of norms in finite dimensional spaces and the properties of the bubble functions, one can show that

$$\left\|r_{T_h}^B\right\|_{L^2(T_h)}^2 \approx \int_{T_h} r_{T_h}^B \phi_{T_h} \,\mathrm{d}x \qquad \text{and} \qquad \left\|r_{F_h}^B\right\|_{L^2(F_h)}^2 \approx \int_{F_h} r_{F_h}^B \phi_{F_h} \,\mathrm{d}s, \tag{4.15}$$

$$\left\|\phi_{T_h}\right\|_{L^2(T_h)} \lesssim \left\|r_{T_h}^B\right\|_{L^2(T_h)} \qquad \text{and} \qquad \left\|\phi_{F_h}\right\|_{L^2(\omega_{F_h})} \lesssim h_{F_h}^{1/2} \left\|r_{F_h}^B\right\|_{L^2(F_h)}. \tag{4.16}$$

Details can be found in [Ver96, Ver13, BC04]. To estimate $r_{T_h}^B$, we use (1.1) on the curved element $T \in \mathcal{T}$ corresponding to $T_h \in \mathcal{T}_h$. When integrating by parts, the boundary terms vanish due to the bubble functions. We get

$$\begin{aligned}\left\|r_{T_h}^B\right\|_{L^2(T_h)}^2 \lesssim \int_{T_h} -\nabla u_h \cdot \nabla \phi_{T_h} - u_h \phi_{T_h} \,\mathrm{d}x + \int_{T_h} f_h \phi_{T_h} \,\mathrm{d}x \\ + \int_T \nabla u \cdot \nabla \phi_{T_h}^\ell + u \phi_{T_h}^\ell \,\mathrm{d}x - \int_T f \phi_{T_h}^\ell \,\mathrm{d}x.\end{aligned}$$

For the integrals over T_h, we insert the according integrals over T and apply Lemma 3.5

$$\begin{aligned}\left\|r_{T_h}^B\right\|_{L^2(T_h)}^2 \lesssim \int_T \nabla(u - u_h^\ell) \cdot \nabla \phi_{T_h}^\ell + (u - u_h^\ell)\phi_{T_h}^\ell \,\mathrm{d}x + \int_T (f_h^\ell - f)\phi_{T_h}^\ell \,\mathrm{d}x \\ + \lambda_\Gamma(T) \left(\|\nabla u_h\|_{L^2(T_h)} \|\nabla \phi_{T_h}\|_{L^2(T_h)} + \|u_h - f_h\|_{L^2(T_h)} \|\phi_{T_h}\|_{L^2(T_h)} \right).\end{aligned}$$

We apply the Cauchy-Schwarz inequality and then use Lemma 3.6 for the inverse lifting of $\left\|\phi_{T_h}^\ell\right\|_{L^2(T)}$. Then, an inverse inequality and (4.16) yield

$$\begin{aligned}\left\|r_{T_h}^B\right\|_{L^2(T_h)} \lesssim h_{T_h}^{-1} \left(\left\|u - u_h^\ell\right\|_{H^1(T)} + \operatorname{osc}(f, T) \right) \\ + \lambda_{\Gamma_h}(T) \left(h_{T_h}^{-1} \|\nabla u_h\|_{L^2(T_h)} + \|u_h - f_h\|_{L^2(T_h)} \right).\end{aligned}$$

On the inner facets $F \in \mathcal{F}_h \setminus \mathcal{F}_h^\partial$ we proceed similarly. After partial integration, we add (1.1), i.e.

$$\begin{aligned}\left\|r_{F_h}^B\right\|_{L^2(F_h)}^2 &\lesssim \int_{\omega_{F_h}} \Delta u_h \phi_{F_h} \,\mathrm{d}x + \int_{\omega_{F_h}} \nabla u_h \cdot \nabla \phi_{F_h} \,\mathrm{d}x \\ &\lesssim \int_{\omega_{F_h}} (r_{T_h}^B + u_h - f_h)\phi_{F_h} \,\mathrm{d}x + \int_{\omega_{F_h}} \nabla u_h \cdot \nabla \phi_{F_h} \,\mathrm{d}x \\ &\quad + \int_{\omega_F} (f - u)\phi_{F_h}^\ell \,\mathrm{d}x - \int_{\omega_F} \nabla u \cdot \nabla \phi_{F_h}^\ell \,\mathrm{d}x.\end{aligned}$$

Lemma 3.5 leads to

$$\begin{aligned}
\left\|r_{F_h}^B\right\|_{L^2(F_h)}^2 &\lesssim \int_{\omega_{F_h}} r_{T_h}^B \phi_{F_h}\,\mathrm{d}x \;+ \int_{\omega_F} (f - f_h^\ell)\phi_{F_h}^\ell\,\mathrm{d}x \\
&\quad + \int_{\omega_F} \nabla(u_h^\ell - u)\cdot\nabla\phi_{F_h}^\ell + (u_h^\ell - u)\phi_{F_h}^\ell\,\mathrm{d}x \\
&\quad + \lambda_\Gamma(T)\left(\|\nabla u_h\|_{L^2(\omega_{F_h})}\|\nabla\phi_{F_h}\|_{L^2(\omega_{F_h})} + \|u_h - f_h\|_{L^2(\omega_{F_h})}\|\phi_{F_h}\|_{L^2(\omega_{F_h})}\right) \\
&\lesssim \left\|r_{T_h}^B\right\|_{L^2(\omega_{F_h})}\|\phi_{F_h}\|_{L^2(\omega_{F_h})} \;+ \left\|f - f_h^\ell\right\|_{L^2(\omega_F)}\left\|\phi_{F_h}^\ell\right\|_{L^2(\omega_F)} \\
&\quad + \left\|u_h^\ell - u\right\|_{H^1(\omega_F)}\left\|\phi_{F_h}^\ell\right\|_{H^1(\omega_F)} \\
&\quad + \lambda_\Gamma(T)\left(\|\nabla u_h\|_{L^2(\omega_{F_h})}\|\nabla\phi_{F_h}\|_{L^2(\omega_{F_h})} + \|u_h - f_h\|_{L^2(\omega_{F_h})}\|\phi_{F_h}\|_{L^2(\omega_{F_h})}\right).
\end{aligned}$$

With the Cauchy-Schwarz inequality, Lemma 3.6, an inverse inequality and (4.16), we deduce

$$\begin{aligned}
\left\|r_{F_h}^B\right\|_{L^2(F_h)} &\lesssim \left\|h_{\mathcal{T}_h}^{1/2} r_{T_h}^B\right\|_{L^2(\omega_{F_h})} + \left\|h_{\mathcal{T}_h}^{-1/2}(u^{-\ell} - u_h)\right\|_{H^1(\omega_F)} + \left\|h_{\mathcal{T}_h}^{1/2}(f^{-\ell} - f_h)\right\|_{L^2(\omega_{F_h})} \\
&\quad + \sum_{T_h\in\omega_{F_h}} \lambda_\Gamma(T)\left(h_{\mathcal{T}_h}^{-1/2}\|\nabla u_h\|_{L^2(T_h)} + h_{\mathcal{T}_h}^{1/2}\|u_h - f_h\|_{L^2(T_h)}\right).
\end{aligned}$$

Since $\eta_B = \left\|h_{\mathcal{T}_h} r_{T_h}^B\right\|_{L^2(\mathcal{T}_h)} + \left\|h_{\mathcal{T}_h}^{1/2} r_{F_h}^B\right\|_{L^2(\mathcal{F}_h\setminus\mathcal{F}_h^\partial)}$, combining the previous estimates yields

$$\begin{aligned}
\eta_B &\lesssim \left\|u - u_h^\ell\right\|_{H^1(\Omega)} + \operatorname{osc}(f,\mathcal{T}) + \sum_{T_h\in\mathcal{T}_h} \lambda_\Gamma(T)\left(\|\nabla u_h\|_{L^2(T_h)} + h_{\mathcal{T}_h}\|u_h - f_h\|_{L^2(T_h)}\right). \\
&\lesssim |||(u - u_h^\ell, v - v_h^\ell)||| + \operatorname{osc}_h + h_{\mathcal{T}}\eta_{\mathrm{nc}}^{B,0} + \eta_{\mathrm{nc}}^{B,1}.
\end{aligned}$$

ii) Efficiency of η_C For any boundary face $F_h \in \mathcal{F}_h^\partial$, let

$$r_{F_h}^C := \alpha u_h - \beta v_h + \partial_n u_h \qquad \text{and} \qquad \phi_{F_h} := b_{F_h}\, r_{F_h}^C.$$

Then, we estimate as before

$$\begin{aligned}
\left\|r_{F_h}^C\right\|_{L^2(F_h)}^2 &\lesssim \int_{F_h} r_{F_h}^C\phi_{F_h}\,\mathrm{d}s - \int_F (\alpha u - \beta v + \partial_n u)\,\phi_{F_h}^\ell\,\mathrm{d}s \\
&\lesssim \int_{T_h}(r_{T_h}^B + u_h - f_h)\phi_{F_h}\,\mathrm{d}x + \int_{T_h}\nabla u_h\cdot\nabla\phi_{F_h}\,\mathrm{d}x + \int_{F_h}(\alpha u_h - \beta v_h)\phi_{F_h}\,\mathrm{d}s \\
&\quad - \int_T (u - f)\phi_{F_h}^\ell\,\mathrm{d}x - \int_T \nabla u\cdot\nabla\phi_{F_h}^\ell\,\mathrm{d}x - \int_F(\alpha u - \beta v_h)\phi_{F_h}^\ell\,\mathrm{d}s \\
&\lesssim \left(\left\|r_{T_h}^B\right\|_{L^2(T_h)} + \left\|f - f_h^\ell\right\|_{L^2(T)}\right)\|\phi_{F_h}\|_{L^2(T)} \;+ \left\|u - u_h^\ell\right\|_{H^1(T)}\|\phi_{F_h}\|_{H^1(T)} \\
&\quad + \left\|\alpha(u_h^\ell - u) - \beta(v_h^\ell - v)\right\|_{L^2(F)}\left\|\phi_{F_h}^\ell\right\|_{L^2(F_h)} \\
&\quad + \lambda_\Gamma(F)\Big(\|u_h - f_h\|_{L^2(T_h)}\|\phi_{F_h}\|_{L^2(T_h)} + \|\nabla u_h\|_{L^2(T_h)}\|\nabla\phi_{F_h}\|_{L^2(T_h)} \\
&\qquad + \|(\alpha u_h - \beta v_h)\|_{L^2(F_h)}\|\phi_{F_h}\|_{L^2(F_h)}\Big).
\end{aligned}$$

A trace inequality and an inverse estimate yield $\|\phi_{F_h}\|_{L^2(F_h)} \lesssim h_{F_h}^{-1/2} \|\phi_{F_h}\|_{L^2(T_h)}$. We conclude as before

$$\begin{aligned}\left\|r_{F_h}^C\right\|_{L^2(F_h)} \lesssim{}& \left\|h_{T_h}^{1/2} r_{T_h}^B\right\|_{L^2(T_h)} + \left\|h_{T_h}^{1/2}(f^{-\ell} - f_h)\right\|_{L^2(T)} + \left\|h_{T_h}^{-1/2}(u^{-\ell} - u_h)\right\|_{H^1(T)} \\ &+ \left\|\alpha(u - u_h^\ell) - \beta(v - v_h^\ell)\right\|_{L^2(F)} \\ &+ \lambda_\Gamma(F)\left(h_{F_h}^{-1/2}\|\nabla u_h\|_{L^2(T_h)} + h_{F_h}^{1/2}\|u_h - f_h\|_{L^2(T_h)} + \|\alpha u_h - \beta v_h\|_{L^2(F_h)}\right).\end{aligned}$$

Due to the properties of the bubble functions, this directly results in the estimate

$$\begin{aligned}\eta_C &= \left\|h_{\mathcal{F}_h^\partial}^{1/2} r_{F_h}^C\right\|_{L^2(\mathcal{F}_h^\partial)} \\ &\lesssim \left\|u - u_h^\ell\right\|_{H^1(\Omega)} + \operatorname{osc}(f, \mathcal{T}) + \left\|h_{\mathcal{F}^\partial}^{1/2}(\alpha(u - u_h^\ell) - \beta(v - v_h^\ell))\right\|_{L^2(\Gamma)} \\ &\quad + \sum_{F_h \in \mathcal{F}_h^\partial} \lambda_\Gamma(F)\left(\|\nabla u_h\|_{L^2(T_h)} + h_{F_h}\|u_h - f_h\|_{L^2(T_h)} + h_{F_h}^{1/2}\|\alpha u_h - \beta v_h\|_{L^2(F_h)}\right). \\ &\lesssim |||(u - u_h^\ell, v - v_h^\ell)||| + \operatorname{osc}_h + h_{\mathcal{T}}\eta_{\text{nc}}^{B,0} + \eta_{\text{nc}}^{B,1} + h_{\mathcal{F}^\partial}^{1/2}\eta_{\text{nc}}^C.\end{aligned}$$

iii) Efficiency of η_S We introduce for $F_h \in \mathcal{F}_h^\partial$ and $E_h \in \mathcal{E}_h^\partial$ the (surface) bubble functions $b_{F_h}^\partial$ with $\operatorname{supp} b_{F_h}^\partial = F_h$ and $b_{E_h}^\partial$ with $\operatorname{supp} b_{E_h}^\partial = \omega_{E_h}^\partial$. For any $F \in {\mathcal{F}_h}^\partial$ and for any $E \in {\mathcal{E}_h}^\partial$, let

$$\begin{aligned} r_{F_h}^S &:= \Delta_{\Gamma_h} v_h + \alpha u_h - (1+\beta) v_h + g_h, & r_{E_h}^S &:= [[\partial_n v_h]], \\ \psi_{F_h} &:= b_{F_h}^\partial\, r_{F_h}^S, & \psi_{E_h} &:= b_{E_h}^\partial\, r_{E_h}^S. \end{aligned}$$

From the properties of the bubble functions, we deduce

$$\begin{aligned} \left\|r_{F_h}^S\right\|_{L^2(F_h)}^2 &\approx \int_{F_h} r_{F_h}^S \psi_{F_h}\,\mathrm{d}s \qquad \text{and} \qquad \left\|r_{E_h}^S\right\|_{L^2(E_h)}^2 \approx \int_{E_h} r_{E_h}^S \psi_{E_h}\,\mathrm{d}\sigma, \\ \|\psi_{F_h}\|_{L^2(F_h)} &\lesssim \left\|r_{F_h}^S\right\|_{L^2(F_h)} \qquad \text{and} \qquad \|\psi_{E_h}\|_{L^2(\omega_{E_h}^\partial)} \lesssim h_{E_h}^{1/2}\left\|r_{E_h}^S\right\|_{L^2(E_h)}. \end{aligned}$$

As before, we integrate (1.1b) and (1.1c) over F and integrate by parts to get

$$\begin{aligned}\left\|r_{F_h}^S\right\|_{L^2(F_h)}^2 \lesssim{}& \int_{F_h} \nabla_{\Gamma_h} v_h \cdot \nabla_{\Gamma_h}\psi_{F_h} + (\alpha u_h - (1+\beta)v_h + g_h)\,\psi_{F_h}\,\mathrm{d}s \\ &- \int_F \nabla_\Gamma v \cdot \nabla_\Gamma \psi_{F_h}^\ell + (\alpha u - (1+\beta)v + g)\,\psi_{F_h}^\ell\,\mathrm{d}s.\end{aligned}$$

With Lemma 3.5, the properties of the bubble function $b_{F_h}^\partial$ and an inverse inequality, we deduce

$$\begin{aligned}\left\|r_{F_h}^S\right\|_{L^2(F_h)} \lesssim{}& h_{F_h}^{-1}\Big(\left\|v_h^\ell - v\right\|_{H^1(F_h)} + \operatorname{osc}(g, F)\Big) + \left\|\alpha(u_h^\ell - u) - \beta(v_h^\ell - v)\right\|_{L^2(F_h)} \\ &+ \lambda_\Gamma(F)\Big(h_F^{-1}\|\nabla_{\Gamma_h} v_h\|_{L^2(F_h)} + \|v_h - g_h\|_{L^2(F_h)} + \|\alpha u_h - \beta v_h\|_{L^2(F_h)}\Big).\end{aligned}$$

Moreover, with the properties of $b^{\partial}_{E_h}$ and Lemma 3.5,

$$\begin{aligned}
\left\|r^S_{E_h}\right\|^2_{L^2(E_h)} &\lesssim \int_{\omega^{\partial}_{E_h}} r^S_{F_h}\psi_{E_h}\,\mathrm{d}s \;+\int_{\omega^{\partial}_{E_h}} \nabla_{\Gamma_h} v_h\cdot\nabla_{\Gamma_h}\psi_{E_h} + (v_h-g_h)\,\psi_{E_h}\,\mathrm{d}s \\
&\quad+\int_{\omega^{\partial}_{E_h}} (\beta v_h-\alpha u_h)\,\psi_{E_h}\,\mathrm{d}s \\
&\lesssim \int_{\omega^{\partial}_{E_h}} r^S_{F_h}\psi_{E_h}\,\mathrm{d}s \;+\int_{\omega^{\partial}_{E}} \nabla_{\Gamma}(v^\ell_h-v)\cdot\nabla_{\Gamma}\psi^\ell_{E_h} + (v^\ell_h-v)\psi^\ell_{E_h}\,\mathrm{d}s \\
&\quad+\int_{\omega^{\partial}_{E}} \big(\beta(v^\ell_h-v)-\alpha(u^\ell_h-u)\big)\,\psi^\ell_{E_h}\,\mathrm{d}s \;+\int_{\omega^{\partial}_{E}} (g-g^\ell_h)\psi^\ell_{E_h}\,\mathrm{d}s \\
&\quad+\sum_{F_h\in\omega^{\partial}_{E_h}} \lambda_\Gamma(F_h)\Big(\,\|\nabla_{\Gamma_h}v_h\|_{L^2(\omega^{\partial}_{E_h})}\,\|\nabla_{\Gamma_h}\psi_{E_h}\|_{L^2(\omega^{\partial}_{E_h})} \\
&\qquad\qquad+\big(\,\|v_h-g_h\|_{L^2(\omega^{\partial}_{E_h})}+\|\alpha u_h-\beta v_h\|_{L^2(\omega^{\partial}_{E_h})}\,\big)\,\|\psi_{E_h}\|_{L^2(\omega^{\partial}_{E_h})}\Big).
\end{aligned}$$

It immediately follows

$$\begin{aligned}
\left\|r^S_{E_h}\right\|_{L^2(E_h)} &\lesssim h_F^{1/2}\left\|r^S_{F_h}\right\|_{L^2(\omega^{\partial}_{E_h})} + h_F^{-1/2}\left\|v^\ell_h-v\right\|_{H^1(\omega^{\partial}_{E})} + h_F^{-1/2}\,\mathrm{osc}(g,\omega^{\partial}_{E_h}) \\
&\quad+h_F^{1/2}\left\|\alpha(u^\ell_h-u)-\beta(v^\ell_h-v_h)\right\|_{L^2(\omega^{\partial}_{E})} \\
&\quad+\sum_{F_h\in\omega^{\partial}_{E_h}}\lambda_\Gamma(F_h)\Big(h_{F_h}^{-1/2}\,\|\nabla_{\Gamma_h}v_h\|_{L^2(F_h)}+h_{F_h}^{1/2}\,\|v_h-g_h\|_{L^2(F_h)} \\
&\qquad\qquad+h_{F_h}^{1/2}\,\|\alpha u_h-\beta v_h\|_{L^2(F_h)}\Big).
\end{aligned}$$

With $\eta_S=\left\|h_{\mathcal{F}_h}r^S_{F_h}\right\|_{L^2(\mathcal{F}^{\partial}_h)}+\left\|h^{1/2}_{\mathcal{F}_h}r^S_{E_h}\right\|_{L^2(\mathcal{E}^{\partial}_h)}$ and the finite overlap of patch elements,

$$\begin{aligned}
\eta_S &\lesssim \left\|v-v^\ell_h\right\|_{H^1(\Gamma)}+\left\|h_{\mathcal{F}}(\alpha(u^\ell_h-u)-\beta(v^\ell_h-v_h))\right\|_{L^2(\Gamma)}+\mathrm{osc}(g,{\mathcal{F}_h}^{\partial}) \\
&\quad+\sum_{F_h\in\mathcal{F}^{\partial}_h}\lambda_\Gamma(F_h)\left(\|\nabla_{\Gamma_h}v_h\|_{L^2(F_h)}+h_{F_h}\,\|\beta v_h-g_h\|_{L^2(F_h)}+h_{F_h}\,\|\alpha u_h-\beta v_h\|_{L^2(F_h)}\right).
\end{aligned}$$

This verifies the claimed statement and completes the proof. □

5 Numerical Experiments

We implemented a finite element method based on the concepts outlined in [ACF99]. The volume grid is described in two arrays: `c4n` contains the coordinates of the nodes and thereby defined the global node indices. `n4e` lists for each element T_h the global nodes indices of the corners and thereby defines local node and face indices. For the surface representation we introduce the additional array `n4f` containing for each surface element $F\in\mathcal{F}^{\partial}$ the global node indices of its corners. In the implementation we do not follow the above convention that within an element the

boundary face has to be labeled last. Instead, there is an array `bdy_face` containing for each $T_h \in \mathcal{T}_h$ either the value 0 for interior elements or the local face index $i \in \{1, \dots, (d+1)\}$ of the boundary face $F_h \subset T_h$.

To compute the $P1$ stiffness matrix in the volume, on each element $T_h \in \mathcal{T}_h$ we need to determine the constant gradient vectors $\nabla\phi_i$ for $i = 1, \dots, (d+1)$. On each surface element $F_h \in \mathcal{F}_h^\partial$ we have to evaluate $\nabla\psi_j$ for $j = 1, \dots, d$. Suppose $F_h \in \mathcal{F}_h^\partial$ and $T_h \in \mathcal{T}_h$ such that $F_h \subset T_h$. Let $\sigma \in \{1, \dots, (d+1)\}$ denote the local face index of the boundary face F_h. Then, the outer normal to Γ_h on F_h is

$$n_{F_h} = -\nabla\phi_\sigma^T / |\nabla\phi_\sigma|. \tag{5.1}$$

Within T_h, the corner nodes of $F_h \subset T_h$ have the local indices $i \in \{1, \dots, d+1\} \setminus \sigma$ and the gradients $\nabla\psi_j$, of the surface finite element shape functions are given by

$$\nabla\psi_j = \nabla\phi_{i(j)}^T - (\nabla\phi_{i(j)}^T \cdot n_{F_h})\, n_{F_h} \qquad \text{for } j = 1, \dots, d. \tag{5.2}$$

In the adaptive algorithm, elements are marked for refinement using the indicator

$$\eta_{T_h} := \alpha\eta_{C,T_h} + \alpha\eta_{B,T_h} + \tfrac{1}{4}\beta\eta_{S,T_h} \tag{5.3}$$

where the terms on the right-hand side refer to the error contributions of element $T_h \in \mathcal{T}_h$ to the corresponding estimators defined in (4.8). The elements with the largest values of η_{T_h} are marked for refinement until the marked elements contribute to $3/4$ of the total estimated error. For the mesh refinement, we apply the bisection algorithm of [BS12]. Note that marking a boundary element $T_h \in \mathcal{T}_h$ due to large surface or coupling indicators on $F_h \in \mathcal{F}_h^\partial$ or $F_h \subset T_h$ might not lead to an immediate refinement of the surface element because the refinement edge of T_h might be in the interior of Ω_h.

For uniformly refined grids, the number of degrees of freedom (DoF) in the volume is proportional to h_T^{-3} and the number of DoFs on the surface is proportional to h_F^{-2}. In the following we will call a quantity proportional to h_T or h_F whenever it shows an according dependence on the DoFs in the volume or on the surface, respectively. We set $\alpha = \beta = 1$ in the following experiments.

5.1 Convergence to known regular solution

As a first benchmark, we verify our method with the example from [ER13]. On the unit sphere $\Omega = B_1(0) \subset \mathbb{R}^3$ with boundary $\Gamma = \partial\Omega$, the data f and g are prescribed such that the exact solution of the problem (2.3) is

$$u(x, y, z) = \exp\left(-x(x-1) - y(y-1)\right)\ , \tag{5.4a}$$

$$v(x, y, z) = \exp\left(-x(x-1) - y(y-1)\right)\left[1 + x\,(1-2x) + y\,(1-2y)\right]. \tag{5.4b}$$

The computed solution (u_h, v_h) is plotted in Fig. 2. From Fig. 3 we see that both the uniform and the adaptive refinement yield the same asymptotic behaviour with respect to the number of DoFs. On uniformly refined grids, the $H^1(\Omega)$-error of u_h decreases proportionally to h_T. Likewise, the $H^1(\Gamma)$-error of v_h is proportional to h_F. Examining Fig. 4 confirms that the estimator η_h and its

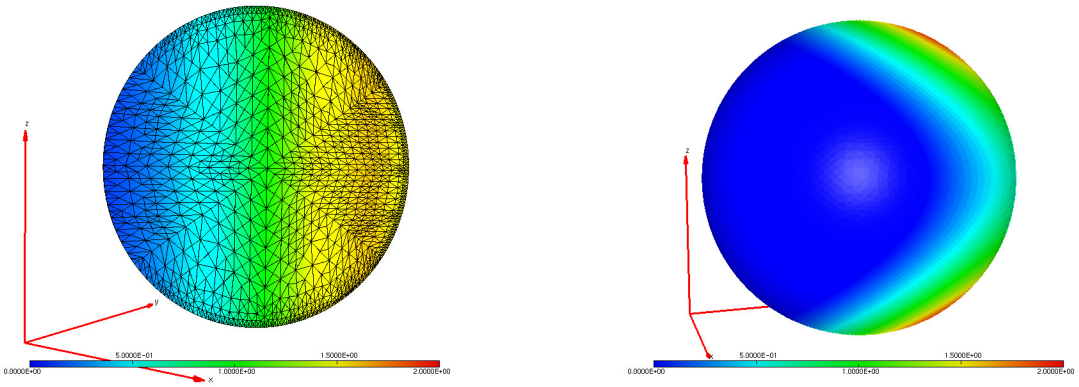

Figure 2: Experiment of Sect. 5.1: cross-section of the solution u_h and the adaptively refined grid (left) and solution v_h on the surface (right).

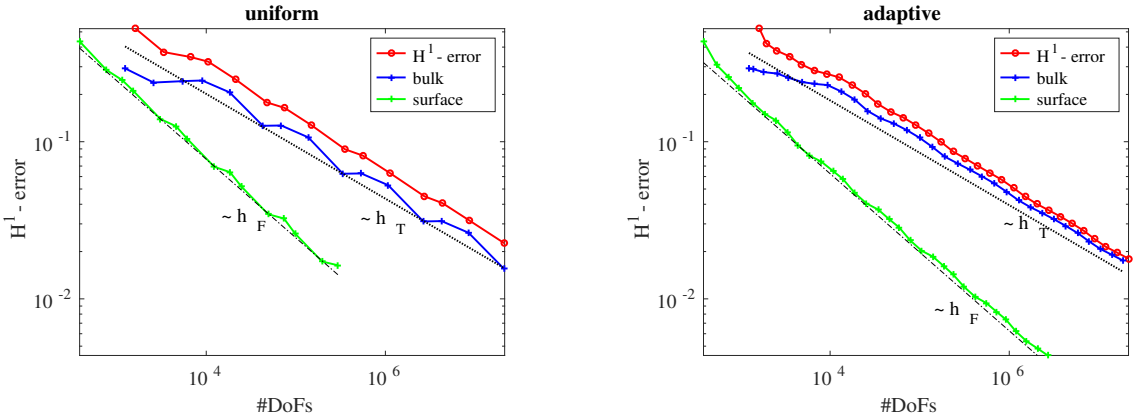

Figure 3: Experiment of Sect. 5.1: Bulk, surface and overall error with respect to the exact solution in the H^1-norm over the number of unknowns for uniform refinement (left) and adaptive refinement (right).

contributions η_B and η_S related to the volume and surface correctly follow the reduction of the overall error and the individual H^1 errors of u_h and v_h, respectively. Moreover, we observe that during the first refinement steps, the estimator η_S of the surface error is dominant, leading to some extra refinement of Γ_h in the adaptive algorithm, cf. Fig. 2. Due to the high regularity of the prescribed solution, the later refinement steps are almost uniform. The estimate η_C of the coupling error is at least about one order of magnitude smaller than the other error contributions and thus does not have any influence on the refinement.

5.2 Non-smooth boundary and grid adaption due to data

In the next experiment with $\Omega = [-1, 1]^3$, we want to examine the effect of a domain Ω with non-smooth boundary Γ and the ability of the adaptive algorithm to resolve singularities of the solution. Then, the surface Γ is only piecewise smooth. Since all faces are flat (i.e. affine), the discretisation of the surface $\Gamma_h = \Gamma$ is exact and hence $\lambda_\Gamma = 0$. We set

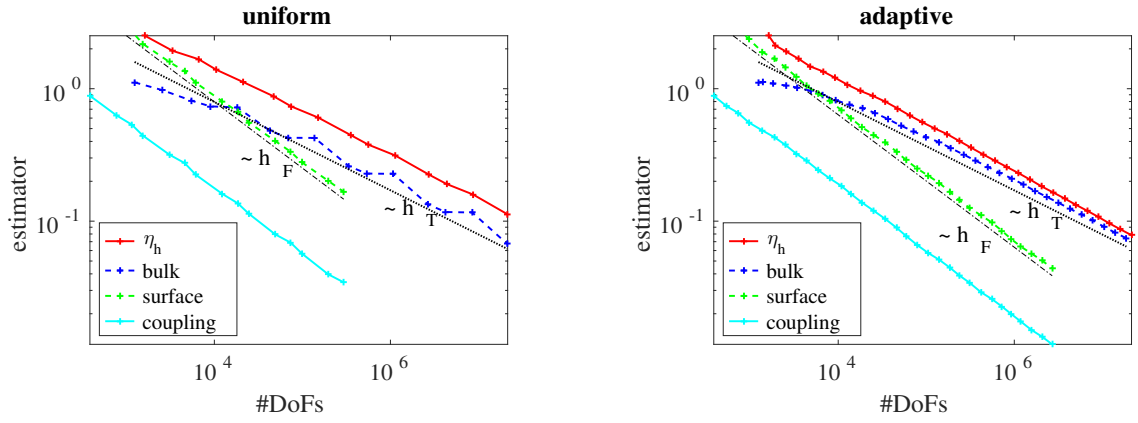

Figure 4: Experiment of Sect. 5.1: Discretisation error estimator η_h with contributions η_B, η_S, η_C over the number of unknowns with uniform refinement (left) and adaptive refinement (right).

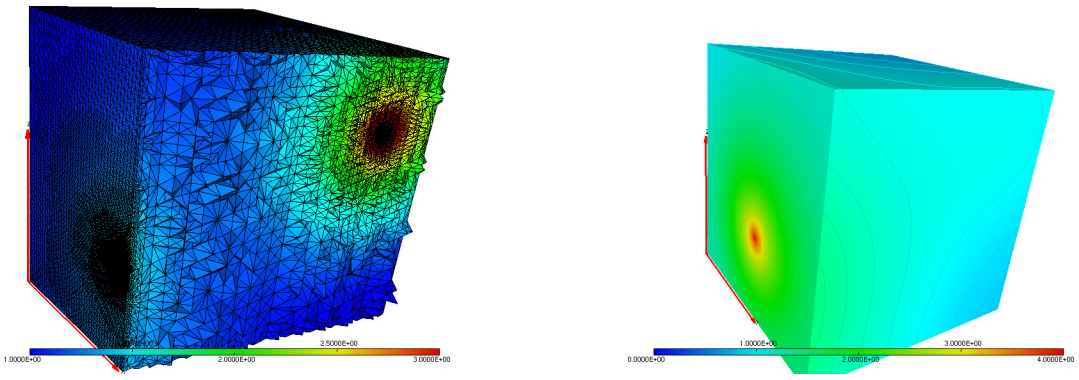

Figure 5: Experiment of Sect. 5.2: Solution for data specified by (5.5): Cross-section of u_h with the locally refined grid (left) and v_h (right).

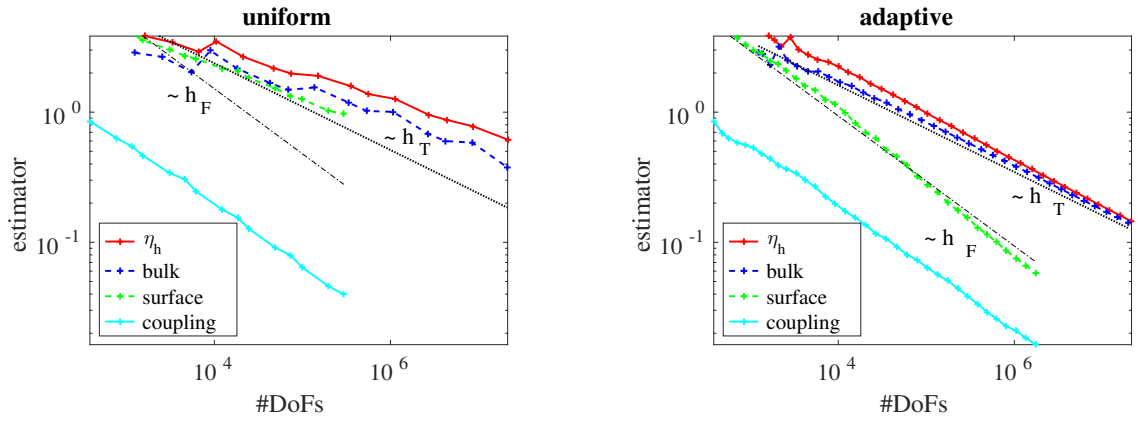

Figure 6: Experiment of Sect. 5.2: Uniform refinement leads to a reduction rate of the estimated error η_h slower than $O(h_T)$ in the volume and $O(h_F)$ on the surface (left) whereas for the adaptively refined grids, η_h meets the optimal rates (right).

$$x_f := (0.7, 0.6, 0.5)\,, \qquad f(x) := (|x - x_f|^2 + 10^{-4})^{-1}\,, \tag{5.5a}$$

$$x_g := (0.1, -1.0, -0.3)\,, \qquad g(x) := (|x - x_g|^{3/2} + 10^{-5})^{-1}\,. \tag{5.5b}$$

By this, we introduce "weak singularities" in Ω and on Γ. The computed solution is plotted in Fig. 5 with a cross-section of the bulk solution u_h on the left-hand side. Fig. 6 shows that adaptive refinement leads to reduction rates of η_B and η_S proportional to $O(h_T)$ and $O(h_F)$, respectively, whereas for uniform refinement the reduction rates are lower and do not reach the same asymptotic behaviour. In particular, we see in Fig. 6, that using uniform refinement the reduction of the surface estimate η_S is considerably slower than $O(h_F)$ while for η_B the difference to the $O(h_T)$ rate is less pronounced. Keeping in mind that the volume grid has more DoFs than the according surface grid, we observe that in each uniform refinement step, the indicator η_S on the surface is larger than η_B in the volume. As before, the coupling error η_C is only marginal with regard to η. Moreover, we see from Fig. 5 that the adaptive algorithm has refined the grid towards the weak singularities of the data. These singularities are well separated from the non-smooth edges of Γ where no extra refinement of the grid can be observed.

5.3 Domain with corner singularities

In the final experiment we examine the effect of corner singularities. Note that the classical example of a reentrant corner and $u(r, \phi) = r^\alpha \sin(\alpha\phi)$ can not be transferred to the coupled problem (1.1). Let the domain Ω be given by a ball of radius 1 where one octant is removed, see Fig. 7. We expect u and v to be of low regularity at the reentrant corner points of the domain Ω and the surface Γ, respectively. We set $x_1 = \frac{1}{2}(-1, 1, 1)$, $x_2 = \frac{1}{2}(1, -1, 1)$, $x_3 = \frac{1}{2}(1, 1, -1)$, and choose

$$f(x) = 0\,, \tag{5.6a}$$

$$g(x) = 20 - 20\big(|x| - \exp(-4|x - x_1|^2) - \exp(-4|x - x_2|^2) + \exp(-4|x - x_3|^2)\big)\,. \tag{5.6b}$$

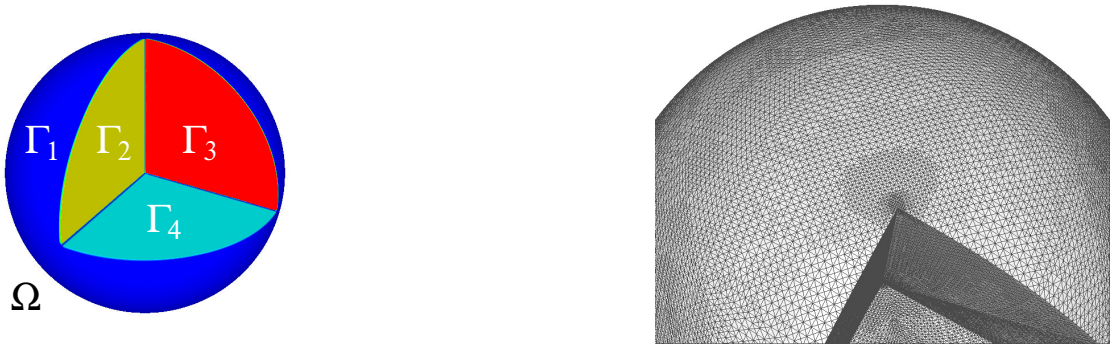

Figure 7: Experiment of Sect. 5.3: The domain Ω with the surface patches Γ^i, $i = 1, 2, 3, 4$ (left). Refinement of the grid towards the corner at the north pole $(0, 0, 1)$ due to the adaptive algorithm (right).

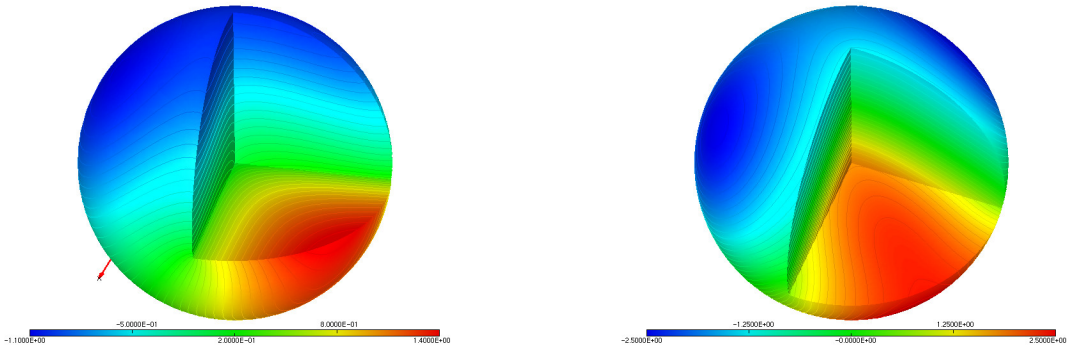

Figure 8: Experiment of Sect. 5.3: Solution u_h (left) and v_h (right).

The computed solution (u_h, v_h) is plotted in Fig. 5.3.

Similar to the experiment of Sect. 5.2, we conclude from Fig. 9 that adaptive refinement leads to reduction rates of η_B and η_S proportional to $O(h_T)$ and $O(h_F)$, respectively, whereas for uniform refinement the reduction rates are lower and do not reach the same asymptotic behaviour. However, when compared to Fig. 6, the deviation of η_S from the $O(h_F)$ line is considerably less pronounced in this experiment. This indicates that for the coupled system, the geometrically induced singularities are weaker than those known in the pure volume or the pure surface problem. At least, it is not possible to trigger stronger singularities using data (5.6).

References

[ACF99] J. Alberty, C. Carstensen, and S.A. Funken. Remarks around 50 lines of matlab: short finite element implementation. *Numerical Algorithms*, 20(2-3):117–137, 1999.

[AO00] M. Ainsworth and J.T. Oden. *A posteriori error estimation in finite element analysis*. Pure and Applied Mathematics (New York). Wiley-Interscience [John Wiley & Sons], New York, 2000.

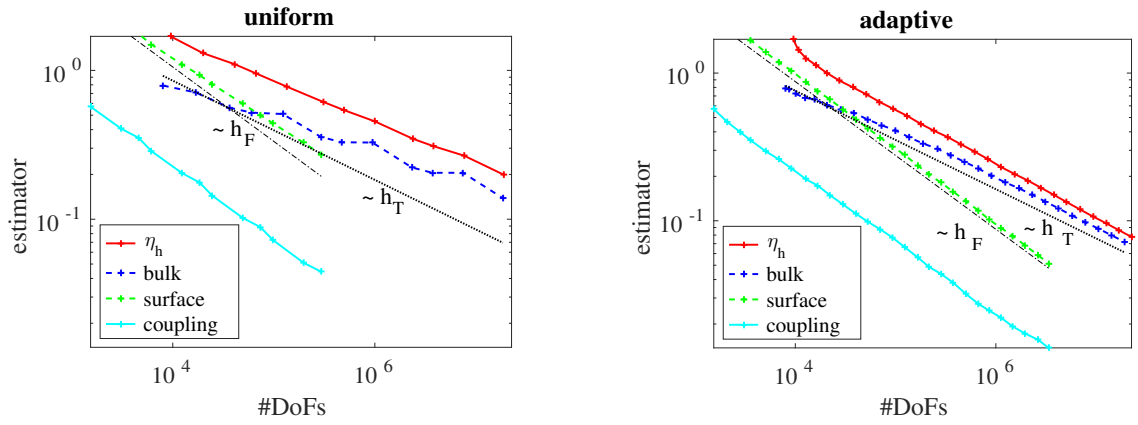

Figure 9: Experiment of Sect. 5.3: Uniform refinement leads to a reduction rate of the estimated error η_h and the volume and surface contributions η_B and η_S slower than $O(h_T)$ and $O(h_F)$, respectively (left). For the adaptively refined grids η_h, the optimal rates are attained (right).

[BC04] Susanne C Brenner and Carsten Carstensen. Finite element methods. *Encyclopedia of computational mechanics*, 2004.

[BCMN13] A. Bonito, J. M. Cascón, P. Morin, and R. H. Nochetto. AFEM for geometric PDE: the Laplace-Beltrami operator. In *Analysis and Numerics of Partial Differential Equations*, pages 257–306. Springer, 2013.

[Ber89] C. Bernardi. Optimal finite-element interpolation on curved domains. *SIAM J. Numer. Anal.*, 26(5):1212–1240, 1989.

[BHLZ14] E. Burman, P. Hansbo, M. G. Larson, and S. Zahedi. Cut finite element methods for coupled bulk-surface problems. *preprint arXiv:1403.6580*, 2014.

[BR78] I. Babuška and W. C. Rheinboldt. A-posteriori error estimates for the finite element method. *Int. J. Numer. Meth. Engng.*, 12(10):1597–1615, 1978.

[BS12] S. Bartels and P. Schreier. Local coarsening of simplicial finite element meshes generated by bisections. *BIT*, 52(3):559–569, 2012.

[CEHL12] C. Carstensen, M. Eigel, R.H.W. Hoppe, and C. Löbhard. A review of unified a posteriori finite element error control. *Numer. Math. Theor. Meth. Appl.*, 5(4):509–558, 2012.

[DD07] A. Demlow and G. Dziuk. An adaptive finite element method for the LaplaceâĂŞBeltrami operator on implicitly defined surfaces. *SIAM J. Numer. Anal.*, 45(1):421–442, 2007.

[Dem09] A. Demlow. Higher-order finite element methods and pointwise error estimates for elliptic problems on surfaces. *SIAM J. Numer. Anal.*, 47(2):805–827, 2009.

[DR98] W. Dörfler and M. Rumpf. An adaptive strategy for elliptic problems including a posteriori controlled boundary approximation. *Math. Comp.*, 67(224):1361–1382, 1998.

[Dub90] F. Dubois. Discrete vector potential representation of a divergence-free vector field in three-dimensional domains: Numerical analysis of a model problem. *SIAM J. Numer. Anal.*, 27(5):1103–1141, 1990.

[Dzi88] G. Dziuk. Finite elements for the Beltrami operator on arbitrary surfaces. In S. Hildebrand and R. Leis, editors, *Partial Differential Equations and Calculus of Variations*, number 1357 in Lecture Notes in Mathematics, pages 142–155. Springer, 1988.

[EFPT15] H. Egger, K. Fellner, J.-F. Pietschmann, and B.Q. Tang. A finite element method for volume-surface reaction-diffusion systems. *Preprint*, IGDK-2015-26, 2015.

[ER13] C.M. Elliott and T. Ranner. Finite element analysis for a coupled bulk-surface partial differential equation. *IMA J. Num. Anal.*, 33(2):377–402, 2013.

[GEW+15] W. Giese, M. Eigel, S. Westerheide, C. Engwer, and E. Klipp. Influence of cell shape, inhomogeneities and diffusion barriers in cell polarization models. *Phys. Biol.*, (to appear), 2015.

[NGC+07] I. L. Novak, F. Gao, Y.-S. Choi, D. Resasco, J. C. Schaff, and B. M. Slepchenko. Diffusion on a curved surface coupled to diffusion in the volume: Application to cell biology. *JCP*, 226(2):1271–1290, 2007.

[RR12] A. Rätz and M. Röger. Turing instabilities in a mathematical model for signaling networks. *J. Math. Biol.*, 65(6-7):1215–1244, 2012.

[Sco73] L. R. Scott. *Finite element techniques for curved boundaries*. PhD thesis, Massachusetts Institute of Technology, 1973.

[SZ90] L. R. Scott and S. Zhang. Finite element interpolation of nonsmooth functions satisfying boundary conditions. *Math. Comp.*, 54(190):483–493, 1990.

[Ver96] R. Verfürth. *A review of a posteriori error estimation and adaptive mesh-refinement techniques*. Wiley-Teubner, 1996.

[Ver13] Rüdiger Verfürth. *A posteriori error estimation techniques for finite element methods*. Oxford University Press, 2013.

[Zlá73] M. Zlámal. Curved elements in the finite element method. i. *SIAM J. Numer. Anal.*, 10(1):229–240, 1973.